Sedimentology (2020) doi: 10.1111/sed.12782

Sedimentology of the continental end-Permian extinction event in the Sydney Basin, eastern Australia

CHRISTOPHER R. FIELDING* (D), TRACY D. FRANK*, ALLEN P. TEVYAW*, KATARINA SAVATIC*, VIVI VAJDA†, STEPHEN MCLOUGHLIN†, CHRIS MAYS†, ROBERT S. NICOLL‡, MALCOLM BOCKING§ and JAMES L. CROWLEY¶

*Department of Earth & Atmospheric Sciences, University of Nebraska-Lincoln, 126 Bessey Hall, Lincoln, NE 68588-0340, USA (E-mail: cfielding2@unl.edu)

†Department of Palaeobiology, Swedish Museum of Natural History, Box 50007, S-104 05, Stockholm, Sweden

‡72 Ellendon Street, Bungendore, NSW 2621, Australia

§Bocking Associates, 8 Tahlee Close, Castle Hill, Bungendore, NSW 2154, Australia

¶Isotope Geology Laboratory, Boise State University, 1910 University Drive, Boise, ID, 83725-1535, USA

Associate Editor - Massimiliano Ghinassi

ABSTRACT

Upper Permian to Lower Triassic coastal plain successions of the Sydney Basin in eastern Australia have been investigated in outcrop and continuous drillcores. The purpose of the investigation is to provide an assessment of palaeoenvironmental change at high southern palaeolatitudes in a continental margin context for the late Permian (Lopingian), across the end-Permian Extinction interval, and into the Early Triassic. These basins were affected by explosive volcanic eruptions during the late Permian and, to a much lesser extent, during the Early Triassic, allowing high-resolution age determination on the numerous tuff horizons. Palaeobotanical and radiogenic isotope data indicate that the end-Permian Extinction occurs at the top of the uppermost coal bed, and the Permo-Triassic boundary either within an immediately overlying mudrock succession or within a succeeding channel sandstone body, depending on locality due to lateral variation. Late Permian depositional environments were initially (during the Wuchiapingian) shallow marine and deltaic, but coastal plain fluvial environments with extensive coal-forming mires became progressively established during the early late Permian, reflected in numerous preserved coal seams. The fluvial style of coastal plain channel deposits varies geographically. However, apart from the loss of peat-forming mires, no significant long-term change in depositional style (grain size, sediment-body architecture, or sediment dispersal direction) was noted across the end-Permian Extinction (pinpointed by turnover of the palaeoflora). There is no evidence for immediate aridification across the boundary despite a loss of coal from these successions. Rather, the end-Permian Extinction marks the base of a long-term, progressive trend towards better-drained alluvial conditions into the Early Triassic. Indeed, the floral turnover was immediately followed by a flooding event in basinal depocentres, following which fluvial systems similar to those active prior to the end-Permian Extinction were re-established. The age of the floral extinction is constrained to 252.54 \pm 0.08 to 252.10 \pm 0.06 Ma by a suite of new Chemical Abrasion Isotope Dilution Thermal Ionization Mass Spectrometry U-Pb ages on zircon grains. Another new age indicates that the return to fluvial sedimentation similar to that before the end-Permian Extinction occurred in the basal Triassic (prior to 251.51 ± 0.14 Ma). The character of the surface separating coal-bearing pre-end-Permian Extinction from coalbarren post-end-Permian Extinction strata varies across the basins. In basin-central locations, the contact varies from disconformable, where a fluvial channel body has cut down to the level of the top coal, to conformable where the top coal is overlain by mudrocks and interbedded sandstone—silt-stone facies. In basin-marginal locations, however, the contact is a pronounced erosional disconformity with coarse-grained alluvial facies overlying older Permian rocks. There is no evidence that the contact is everywhere a disconformity or unconformity.

Keywords Australia, end-Permian extinction, fluvial architecture, Permo-Triassic boundary, Sydney Basin.

INTRODUCTION

Studies of past climate transitions greatly assist the evaluation of future conditions in a time of rapid environmental change. The Permo-Triassic boundary (PTB) was marked by major perturbations to the Earth system, including the largest mass extinction of the geological record (Erwin, 2006; Burgess et al., 2014). This interval saw the final assembly of Pangea, the development of extreme continentality, and unprecedented expansion of subtropical arid belts (Kutzbach & Gallimore, 1989; Kiehl & Shields, 2005; Torsvik & Cocks, 2013). Ocean acidification and deoxygenation culminated in the marine end-Permian extinction event (EPE) around 251.9 Ma (Burgess et al., 2014).

Extrusion of the Siberian Traps Large Igneous Province (LIP) is widely invoked as the principal causal mechanism for the EPE, changing global temperatures, pumping large volumes of toxic aerosols and fly ash into the atmosphere, and facilitating extensive wildfires (Renne & Basu, 1991; Campbell et al., 1992; Renne et al., 1995; Bowring et al., 1998; Wignall, 2001; Kamo et al., 2003; Payne & Kump, 2007; Retallack & Jahren, 2008; Svensen et al., 2009; Sobolev et al., 2011; Grasby et al., 2011; Rothman et al., 2014; Burgess & Bowring, 2015; Le Vaillant et al., 2017; Rampino et al., 2017). Terrestrial floras were wiped out, leading to widespread destabilization of continental landscapes, with enhanced rates of soil erosion and sediment runoff (Algeo & Twitchett, 2010; Vajda et al., 2020). Influenced by these findings, many researchers have suggested that sedimentary facies patterns across the EPE or PTB record a rejuvenation of continental drainage systems, and have

interpreted facies patterns to record a change in fluvial style from one recording slow, sluggish streams to that of highly mobile streams that were overloaded with clastic sediment.

The importance of the PTB in global stratigraphy is exemplified by its status as the boundary between the Palaeozoic and Mesozoic eras. Many expressions of the boundary, such as the Global Stratotype Section and Point (GSSP) in China, are within lithologically uniform marine successions, defined by palaeontological and geochemical criteria, and constrained by increasingly precise geochronological data (Yin et al., 2001, 2005; Cao et al., 2002, 2009; Shen et al., 2011; Burgess et al., 2014). Oceanic records have been preferentially targeted because they are perceived as the most stratigraphically complete and likely to preserve globally integrated signals (Algeo et al., 2011). In contrast, many PTB records from non-marine basins are associated with profound changes in palaeoenvironmental conditions, but they are typically less well constrained in absolute time. Nonetheless, an understanding of the EPE in continental settings is crucial to a full appreciation of the global biotic crisis. The continental record is also receiving increasing attention because the short-term impacts of climate change appear to be expressed more severely on land (e.g. Benton & Newell, 2014) and the terrestrial ecosystem's response to abrupt environmental change is most relevant to human societies.

Major biotic changes in both the marine and non-marine systems began well before the end-Permian, at the Guadalupian-Lopingian (middle-upper Permian) boundary (Stanley & Yang, 1994; Isozaki *et al.*, 2007a,b; Rampino & Shen, 2020), although the severity of this early event

has been questioned (Clapham et al., 2009). The onset of the main marine extinction event at 251.941 ± 0.037 Ma, now considered to have occurred shortly before the Permian-Triassic boundary (PTB) at 251.902 \pm 0.024 Ma (Burgess et al., 2014), is also more complex than originally thought. Some marine records indicate a delayed extinction in deep palaeowater depths (Jiang et al., 2015) and other recent work suggests that a second extinction event in the earliest Triassic followed the main kill event (Yin et al., 2007; Song et al., 2013). Retallack et al. (2011) and Retallack (2013) have gone so far as to propose repeated 'greenhouse crises' throughout the late Permian and Early Triassic that cumulatively led to the main crisis and delayed recovery from it. Recently, Fielding et al. (2019) showed that the turnover in continental palaeofloras in the high-palaeolatitude Sydney Basin of eastern Australia occurred some 400 kyr before the marine extinction event, and may have been linked with emissions associated with the primary extrusion phase of the Siberian Traps LIP. New results from other regions of the world appear to support this hypothesis (Gastaldo et al., 2020; Chu et al., 2020).

Facies changes across the PTB in the non-marine realm have been documented by several groups, and are interpreted to record some combination of abrupt warming, aridification, turnover in palaeoflora and palaeofauna, and landscape degradation (Retallack, 1999, 2005; Algeo & Twitchett, 2010; Benton & Newell, 2014; Smith & Botha-Brink, 2014; Bercovici et al., 2015; Winguth et al., 2015; Vajda et al., 2020). Other studies, however, have concluded little or no apparent change in depositional environment or palaeogeography across the PTB and/or EPE, or non-synchronous changes (e.g. McLoughlin et al., 1997; Yu et al., 2007; Yang et al., 2010; Gastaldo et al., 2015; Gastaldo & Neveling, 2016; Fielding et al., 2019; Wignall et al., 2020). The emerging pattern is one of spatial and temporal heterogeneity in the record of the end-Permian palaeoenvironmental crisis on land.

This paper addresses sedimentary facies and other palaeoenvironmental changes across the EPE and PTB in a continental margin setting at high southern palaeolatitudes (60 to 65°S; Torsvik & Cocks, 2013) — the Sydney Basin of eastern Australia (Fig. 1). The findings of this study are indexed to a detailed relative and absolute time model that allows detailed insights into the pacing of events on the Panthalassan margin of

Gondwana and contributes to the growing picture of end-Permian palaeoenvironmental change.

FACIES CHANGES ACROSS THE PERMOTRIASSIC BOUNDARY

Some palaeoenvironmental investigations of the Permo-Triassic transition in continental settings have concluded that wildfires facilitated by high atmospheric oxygen contents, abrupt warming and aridification led to widespread landscape degradation (Retallack, 2005; Glasspool & Scott, 2010; Shen et al., 2011; Yan et al., 2019). Several sedimentological investigations have documented concomitant changes in fluvial style across the boundary (e.g. Newell et al., 1999; Ward et al., 2000; Michaelsen, 2002; Arche & López-Gómez, 2005; Lopez-Gomez et al., 2005; Smith & Botha-Brink, 2014; Zhu et al., 2019; Botha et al., 2020) and attributed them to the same palaeoenvironmental disturbances. A common finding of these investigations has been the interpretation of an abrupt upward change across the boundary from deposits of meandering rivers (a planform style facilitated by vegetated, fine-grained substrates) to those of more mobile, braiding rivers (a planform style facilitated by lack of vegetation and an oversupply of coarse-grained sediment load). Questions nonetheless persist as to the nature of these boundaries, and as to whether the succession was a record of continuous sediment accumulation across the EPE. If the contact were disconformable, there is no way of knowing how long after (or potentially, before) the ecological collapse the change took place without independent geochronological control.

The Karoo Basin of southern Africa, which was a foreland basin in middle to high southern palaeolatitudes (ca 50 to 60°S: Torsvik & Cocks, 2013) during the PTB, has a well-exposed record of continental strata that have been studied extensively. Smith (1995), Ward et al. (2000) and Smith & Botha-Brink (2014) argued that a major change in fluvial style from 'meandering' to 'braided' systems coincides with the EPE (considered equivalent to the PTB) in the Karoo Basin. In effect, this constitutes a change from heterolithic channel fills of limited width that show evidence for systematic lateral accretion processes to sandstone-dominated, sheet-like bodies showing evidence of more stochastic channel mobility. In detail, however, these

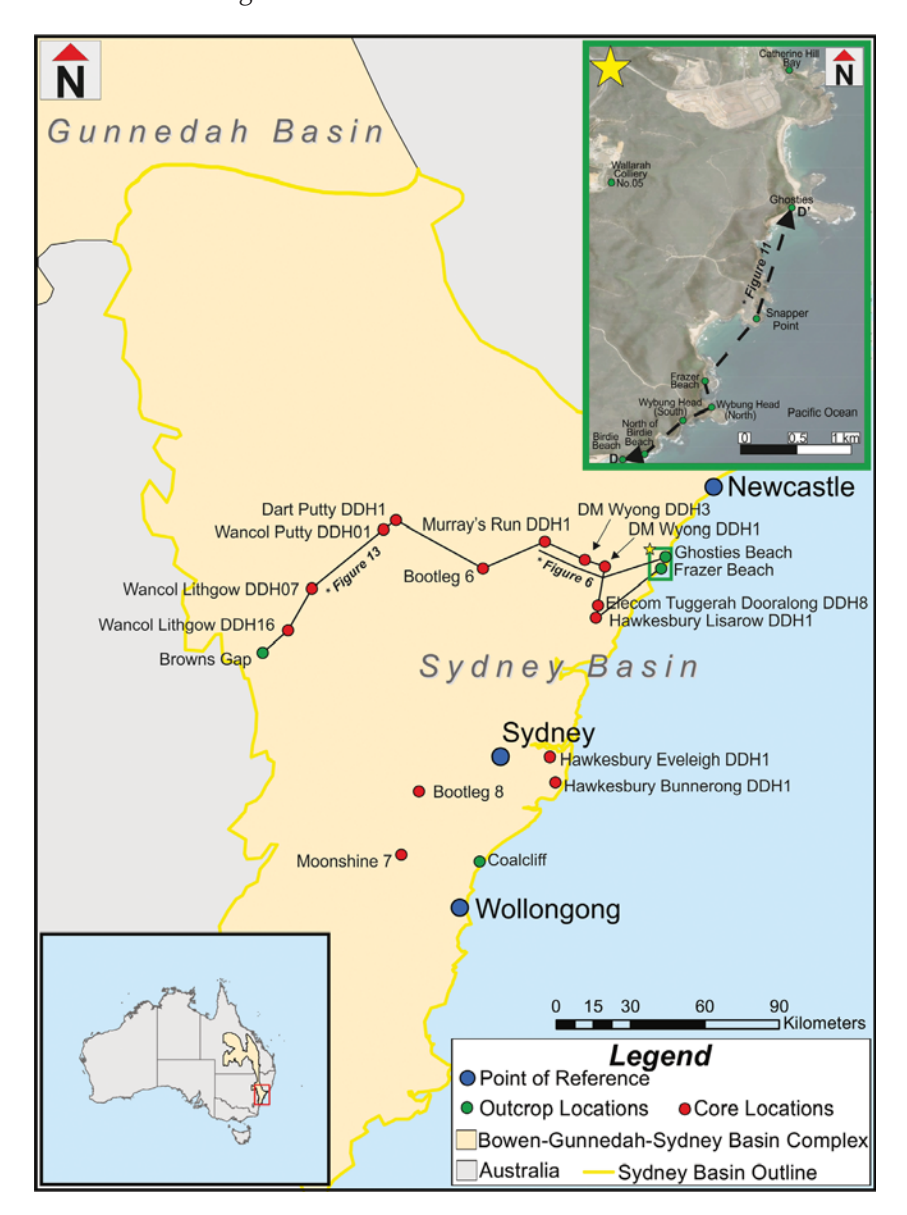


Fig. 1. Maps showing the location of the Sydney Basin in south-east Australia, and of field sites and drillcores examined in this study. Inset image shows locations along the coast south of Newcastle. The lines of cross-section shown in Figs 6, 10 and 12 are indicated.

changes are progressive, and seem to occur in several stages over ca 100 m of vertical section, recording perhaps 120 kyr of time (Smith & Botha-Brink, 2014). Facies changes in the Karoo Basin were attributed by Ward et al. (2000), Smith & Botha-Brink (2014) and Botha et al. (2020) to reflect an increase in sediment load relative to discharge following a catastrophic destruction of plant ecosystems and a change to a warmer, drier, and more seasonal climate at the PTB. There is, however, a dispute over exactly where the EPE and PTB are located within the succession that is not yet fully resolved (Gastaldo et al., 2015, 2018; Gastaldo & Neveling, 2016). Gastaldo et al. (2020) noted that the base of the Lystrosaurus Assemblage Zone (equated with the vertebrate-defined EPE in the Karoo Basin) is at least 300 kyr older than the marine EPE, and significantly pre-dates the transition from mudrock-dominated (Palingkloof Member) to sandstone-dominated (Katberg Formation) successions. Apart from the few radiogenic isotope ages and the palaeomagnetic framework summarized by Gastaldo *et al.* (2020), there is not yet an independent means of assessing the context of the documented palaeoenvironmental changes within a refined chronostratigraphic framework.

Newell *et al.* (1999) documented an abrupt coarsening-upward discontinuity in fluvial successions of the Southern Uralian foreland basin in Russia at or about the PTB, which they interpreted to record a massive rejuvenation in terminal fan systems across the boundary. This is

accompanied by evidence for a drying trend in palaeoclimate from semi-arid/seasonal to arid in mid-northern palaeolatitudes. Here, however, there are no constraints on exactly when this change took place in absolute time, only that the underlying section contains upper Permian fossils, and rocks above the conglomeratic association are Lower Triassic. An abrupt grain-size increase in fluvial facies was also documented by Davies et al. (2010) from the Kuznetsk Basin, Siberia, constrained only by a radiogenic isotopic age of 250.3 \pm 0.7 Ma from a basalt lava a short interval above the change.

In the Bowen Basin of Queensland, eastern Australia, located at 45 to 55°S palaeolatitude (Torsvik & Cocks, 2013), Michaelsen (2002) proposed an abrupt change in fluvial style at the top of the upper Permian Rangal Coal Measures to record palaeoenvironmental upheaval at the PTB, and interpreted a change from large, heterolithic channel fills to a sheet-like sandstone body at the inferred PTB to reflect changing runoff regimes and increased coarse sediment supply across a devegetated landscape. Once again, there are virtually no absolute age constraints on this interpretation, which relies on the 'rule of thumb' that the top of the uppermost coal represents the PTB in eastern Australia. However, what is also unacknowledged is that sheet-like sandstone bodies occur at several stratigraphic levels within the upper Permian Rangal Coal Measures of the Bowen Basin (Fielding et al., 1993; Fielding, 2015) and are not confined to the post-extinction interval. This renders the apparent contrast across the PTB less remarkable.

Fully continental sedimentary successions spanning the Permian-Triassic transition are also represented at very high (70 to 85°S) southern palaeolatitudes, in both the Transantarctic Mountains and the Prince Charles Mountains, Antarctica. At both of these locations, the EPE (marked by the replacement of the Glossopteris flora by a Lepidopteris-Voltziopsis flora, and the appearance of Lystrosaurus remains) corresponds to the loss of coals and an increased proportion of thick multistorev sandstones within the succession (Collinson & Isbell, 1984; Webb & Fielding, 1993; Collinson et al., 1994; McLoughlin et al., 1997; McLoughlin & Drinnan, 1997a, b). However, in most available sections, this contact is scoured, commonly overlain by a microbreccia of reworked clay-pellets (Retallack et al., 2005), and the scarcity of high-resolution radiogenic isotope dates from these successions makes it difficult to resolve the precise timing of

events or to quantify the stratigraphic interval removed by scouring around the EPE (Elliot et al., 2017). Regardless, strata both below and above the EPE were deposited within sandy braided fluvial systems, palaeocurrent directions remain consistent across this horizon and, although disappear. carbonaceous coals mudrocks persist into the lowermost Triassic (Collinson et al., 1994; McLoughlin & Drinnan, 1997a,b).

Documented changes in lithologies and interpreted continental depositional environments across the EPE and PTB in other areas are more complex (e.g. Yu et al., 2007), with examples of both coarsening and fining trends noted. In a palaeo-landward to palaeo-seaward transect in south China (which was in the palaeotropical realm at the time), Bercovici et al. (2015) found an overall decrease in sediment grain size and a record of gradual inundation by standing water environments across the PTB. In a note of caution, however, Bourguin et al. (2018) demonstrated that some of the key sections in this analysis have been compromised by structural deformation. Evidence of short-term flooding or ponding in the landscape directly following the EPE has also been recorded in Queensland, Australia (Wheeler et al., 2020), and in recent work in the Sydney Basin (Vajda et al., 2020).

Clearly, the sedimentological responses to palaeoenvironmental perturbances at or around the PTB were complex and both spatially and temporally variable. The following documents depositional facies and their interpreted formative environments across the PTB and EPE in various locations across the Sydney Basin of eastern Australia, using both outcrop and an extensive inventory of bore cores from exploration drilling. From an analysis of vertical and lateral facies patterns, the evolution of the end-Permian depositional landscape in eastern Australia is interpreted.

THE SYDNEY BASIN OF NEW SOUTH WALES, AUSTRALIA

The Sydney Basin of central eastern New South Wales, Australia, is a south-east-plunging synclinorium preserving a thick (up to 6 km; Mayne et al., 1974) sedimentary succession of Permo-Triassic age (Fig. 1). It is bounded to the west by older Palaeozoic igneous and metasedimentary terrains of the Tasman Orogen, and to the east by the Permo-Triassic New England Orogen (Veevers, 2000; Glen, 2005; Rosenbaum, 2018). The basin opened during a period of geographically widespread but modest crustal extension in the early Permian, was dominated by thermal relaxation during the late early to middle Permian, and later became a retroarc foreland basin during the late Permian in response to crustal contraction associated with the Hunter-Bowen Event (Scheibner, 1973, 1993; Herbert & Helby, 1980; Tye et al., 1996; Holcombe et al., 1997; Fielding et al., 2001; Korsch & Totterdell, 2009). The latter phase of development led to the accumulation of 2 to 3 km of upper Permian to Middle Triassic strata before the basin was closed and compressively deformed in the Middle Triassic (Mayne et al., 1974; Herbert & Helby, 1980). Subsequently, much of the record of the convergent margin orogen (arc, forearc and accretionary prism) has been rifted and is probably now partially preserved as the Lord Howe Rise and parts of New Zealand in the south-west Pacific.

The lower Permian rift fill comprises a heterogeneous array of magmatic, volcaniclastic and terrigenous clastic rocks that varies considerably in thickness and character from place to place. The overlying lower to middle Permian succession comprises terrigenous clastic sedimentary rocks of mainly shallow marine to coastal plain deposits. The upper Permian succession shows a progressive, though not monotonic, change from dominantly shallow marine to dominantly coastal alluvial plain deposits, and this trend continues into the overlying Triassic succession (Herbert & Helby, 1980). A considerable body of sedimentological research has been carried out on the upper Permian and overlying Triassic succession of the Sydney Basin (Fig. 2). Sedimentological analyses of the upper Permian Illawarra Coal Measures in the south were reported by Bamberry (1990) and Bamberry et al. (1995), and of the Triassic succession by Diessel et al. (1967), Ward (1972), Goldbery & Holland (1973), Conaghan et al. (1982), Cowan (1993) and Dehghani (1994). In the northern limb of the basin, the upper Permian Newcastle Coal Measures have been studied sedimentologically by Diessel (1980, 1992), Warbrooke (1981) and Bamberry & Herbert (1996), and more recently by Breckenridge et al. (2019). The overlying Triassic succession has been documented in part by Uren (1980), Cowan (1993) and Bamberry & Herbert (1996).

These studies collectively show that the western margin of the Sydney Basin (including the Illawarra region in the south) shows repeated

onlap of stratal units and erosional truncation, with gradual thinning of component units westward towards the palaeo-Australian craton. On the other hand, the eastern portion of the basin (including the northern Newcastle region) lay close to the foredeep axis during late Permian and Triassic times, and so preserves a much thicker and more stratigraphically complete succession. Published palaeogeographic reconstructions for the late Permian and Triassic of the Sydney Basin (e.g. Herbert & Helby, 1980; Cowan, 1993; Fielding et al., 2001) show a dominance of broadly southward (basin-axial) sediment dispersal in fluvial systems both below and above the Permo-Triassic boundary, with a component of transverse supply from the east in the depocentre and from the west along the cratonic margin. These reconstructions, however, are based on the premise that present structural boundaries (such as the Hunter-Mooki Thrust Fault, which defines the eastern basin edge) were in their present locations during the late Permian and that the preserved basin geometry records its faithfully original geometry. Palaeocurrent data and facies patterns suggest that neither of these assumptions is valid. Furthermore, now-isolated Permian and Triassic outliers in the southern New England Orogen, such as the Cranky Corner and Gloucester Synclines and the Lorne Basin, preserve a stratigraphy that can be correlated with that of the adjacent Hunter Valley and Newcastle coalfields (Moloney et al., 1991; Weber & Smith, 2001; Facer & Foster, 2003; Pratt, 2010), suggesting that in the Permian and earliest Triassic the depositional surface of the Sydney Basin included much of what was subsequently deformed to constitute the southern New England Orogen. New palaeogeographic maps (Fig. 3) for the late and latest Permian, and earliest Triassic, take this into account.

The upper Permian succession throughout the Sydney Basin is rich in coal resources and has supported a profitable mining industry for over 200 years. A legacy of this activity is a rich inventory of geological data, including many hundreds of fully cored boreholes together with surface and underground mining records. Additionally, the upper Permian succession crops out along the coast both north of Wollongong on the southern limb of the basin (Illawarra Coalfield) and south of Newcastle on the northern limb (Newcastle Coalfield; Fig. 1). More scattered surface exposures are also accessible in the west, along the margins of the Blue

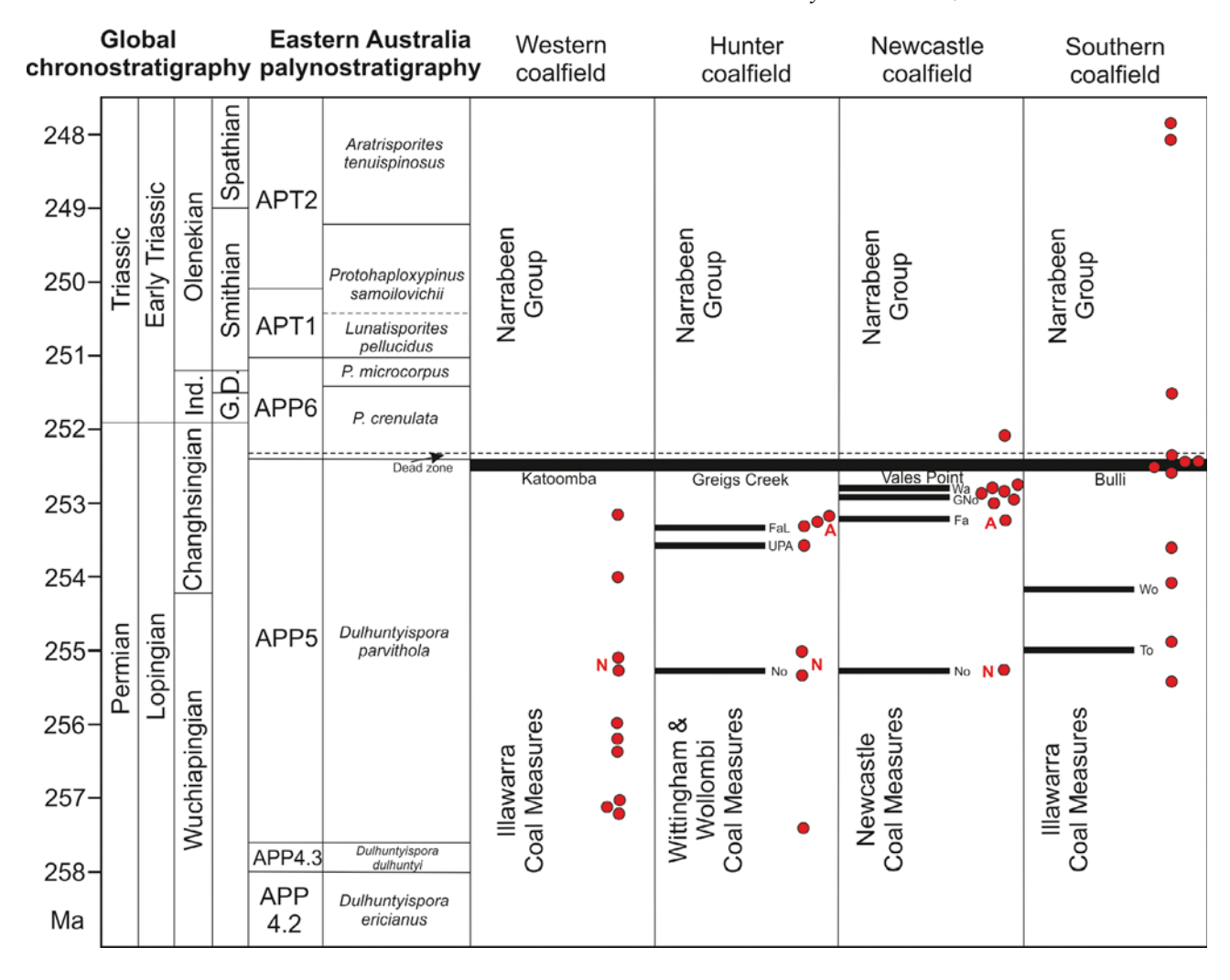


Fig. 2. Stratigraphic framework diagram showing global chronostratigraphy (Ogg et al., 2016), eastern Australian palynostratigraphy (Laurie et al., 2016, updated by Mays et al., 2020), and stratigraphic nomenclature in different parts of the Sydney Basin (Coalfield Council of New South Wales, 1999). The distribution of new, high-precision CA-IDTIMS U-Pb absolute ages (red spots: Metcalfe et al., 2015; Fielding et al., 2019, ages documented herein, and R.S. Nicoll, unpublished data) is given along with relevant coal seams. G – Griesbachian, D – Dienierian, No – Nobby's Coal, UPA – Upper Pilot A coal, FaL – Fassifern Lower coal, Fa – Fassifern coal, GNo – Great northern coal, Wa – Wallarah coal, To – Tongarra coal, Wo – Wongawilli coal. N – Nobbys Tuff, A – Awaba Tuff. The 'Dead Zone' refers to an interval immediately the uppermost Permian coal seam from which all elements of the Permian Glossopteris flora are missing, and in which only charcoal and rare palynomorphs are preserved (Vajda et al., 2020; Mays et al., 2020).

Mountains Plateau (Western Coalfield). This study utilizes a combination of outcrop and subsurface data, emphasizing the excellent coastal exposures north of Wollongong and south of Newcastle, along with numerous fully cored boreholes (Fig. 1).

METHODS

Surface exposures were examined in the field, and vertical sections measured at accessible locations.

Where exposures could not be accessed directly, vertical intervals were measured with a laser range-finder. Drillcores from strategically located bore-holes were accessed at the New South Wales Department of Minerals and Energy W.B. Clarke Geoscience Information Center at Londonderry, western Sydney. Selected cores were sampled for carbon-isotope geochemistry and palynological analysis. Some cores were also sampled for possible geochronological analysis using the Chemical Abrasion Isotope Dilution Thermal Ionization Mass Spectrometry (CA-ID-TIMS) U-Pb method.

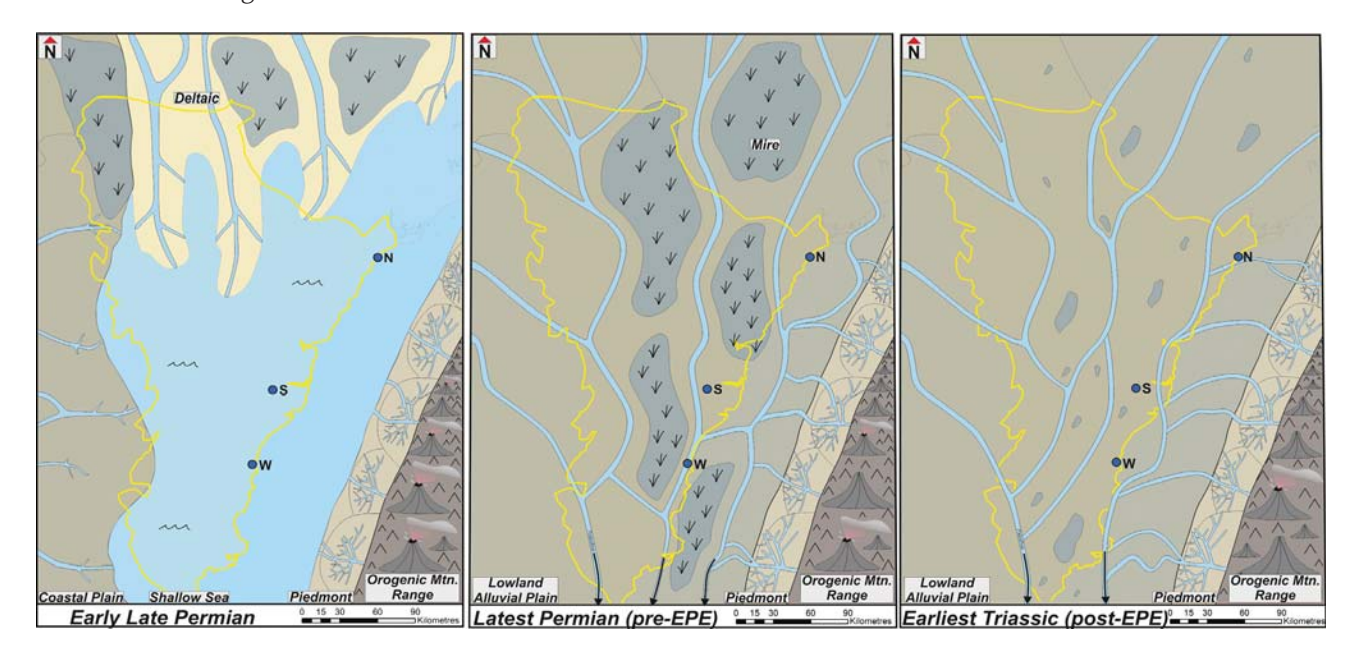


Fig. 3. Palaeogeographic maps showing interpreted sediment dispersal patterns for: (i) Late Permian; (ii) Latest Permian; and (iii) Early Triassic of the Sydney Basin, New South Wales. These maps are generalized but are informed by a large body of facies and palaeoflow data from locations distributed around the basin (see Fig. 12 for palaeoflow data). A major premise behind the maps is that the New England Orogen (NEO) to the north-east of the basin did not yet exist at this time, as evidenced by the preservation of thick Permian successions in NEO outliers such as the Cranky Corner and Gloucester areas, where the stratigraphy can be correlated in detail with that of the adjacent Sydney Basin. In the early late Permian, a shallow sea in the south was progressively filled, giving rise to an extensive coastal plain. In the latest Permian, continued regression led to the formation of a coastal alluvial plain across the entire basin. Following the end-Permian Extinction (EPE), the coastal alluvial plain was reestablished with one or more episodes of ponding of the water table giving rise to widespread development of shallow floodbasins. W – Wollongong, S – Sydney, N – Newcastle.

Lateral continuity of beds was traced physically at outcrop, and in the subsurface was traced by construction of cross-sections. Subsurface mapping is facilitated by the presence of many distinctive, laterally persistent, stratigraphic markers in the Permian succession, particularly coal seams with distinctive internal stratigraphies, and tuff beds, some of which are many metres thick. The following section establishes the range of lithofacies recognized in the uppermost Permian to lowermost Triassic succession. It is noteworthy that a strongly overlapping array of lithofacies accounts for the interval both below and above the EPE and PTB.

To assess temporal variations in sediment provenance that could impact weathering indices, thin sections were prepared from six sandstone samples spanning the stratigraphic interval of interest in the Hawkesbury Bunnerong-1 (PHKB1) drill core, which is situated in the depocentre of the Sydney Basin (Fielding et al., 2019). Thin sections were analyzed for mineralogy, sedimentary textures and diagenesis

using transmitted light microscopy. Point counting of framework grains was conducted on each sample using a standard petrographic microscope as outlined by Harwood (1988). Quartz, feldspar and lithic grain abundances in each sample were used to determine sandstone type (Folk, 1980) and assess provenance (Dickinson, 1983). In these analyses, quartz refers to monocrystalline quartz, whereas chert and polycrystalline quartz grains are counted as lithic fragments.

The $\delta^{13}C_{org}$ values of bulk sedimentary organic matter in coal, mudrock and sandstone were analyzed using a Costech Elemental Analyzer (Costech Analytical Technologies Inc., Valencia, CA, USA) connected to a Thermo Finnigan MAT 253 Isotope Ratio Mass Spectrometer (ThermoFisher Scientific, Waltham, MA, USA) at the Keck-NSF Palaeoenvironmental and Environmental Laboratory, University of Kansas. Prior to analysis, samples were powdered using a Siebtechnik rock pulveriser (Siebtechnik Tema B.V., Rijswijk, The Netherlands) and acidified in

1 N HCl for 24 h to remove inorganic carbon. Quality control was monitored using working standards DORM and ATP. Reported in per mil (%) relative to the Vienna PeeDee Belemnite (VPDB) standard, $\delta^{13}C_{org}$ values were reproducible to better than $\pm 0.13\%$ (1σ SD).

Fourteen palynological samples were collected from the outcrop exposures at Coalcliff, New South Wales (34°15′18.9″S, 150°58′22.2″E). Palynological samples were processed following the methods outlined by Fielding et al. (2019). Three samples were barren of identifiable palvnomorphs (S029704 to S029706); three additional samples had poor palynomorph recovery (<100 palynomorphs across two slides (S029707 to S029709). Palynofacies data were collected from all samples. Palvnostratigraphic correlations were based on regional biostratigraphic schemes (Price, 1997; Laurie et al., 2016; Mays et al., 2020). All palynological slides are housed at the Department of Palaeobiology, Swedish Museum of Natural History, Stockholm, Swe-

A large number of samples of putative tuffaceous mudrocks and tuffs were processed for zircon at the Boise State University Isotope Geology Laboratory. Some contain no zircon and others contain large populations of physically abraded zircons that indicate a detrital origin. Some samples also contain small populations of sharply faceted grains that are potentially of first-cycle volcanic origin. Only sharply faceted grains were mounted for Laser Ablation Inductively Coupled Mass Spectrometry (LA-ICPMS) to identify the youngest grains. These young grains were then removed from the mounts and dated using CA-ID-TIMS. Due to the large populations of detrital zircon, with only a few grains of possible primary origin per sample, reported dates are considered as possibly Maximum Depositional Ages, and not Depositional Ages. Complete details of analytical procedures and results are given in Data S1.

FACIES ANALYSIS

An array of nine facies associations (FAs) has been recognized in the uppermost Permian to lowermost Triassic succession of the Sydney Basin in this study (Table 1). These FAs record a range of lowland to coastal alluvial plain channels, levées, floodbasins, lakes, mires and pyroclastic fallout. With the exception of FA H (mire deposits, which are restricted to the Permian)

and FA G (lacustrine), all other FAs occur in both Permian and Triassic successions.

Facies Association A — Description

Facies Association A (FA A) comprises bodies of pebble to cobble conglomerate with subordinate gravelly sandstone <50 m thick but typically <25 m thick (Table 1, Fig. 4). FA A is preserved most abundantly in the Newcastle Coalfield, which, as noted previously, is located close to the foredeep axis of the latest Permian. These bodies occupy linear belts up to a few kilometres wide that are mostly elongate in a south/south-westerly orientation, consistent with palaeoflow data collected from outcrops of those bodies (Fig. 5). They occur at numerous stratigraphic levels within the studied succession, and in many cases are parts of composite bodies comprising storeys of both FAs A and B (Fig. 6). Mapping shows that many such bodies in the Permian succession are enclosed within coal seam splits (for example, Upper Teralba Conglomerate; Fig. 6), and they are offset from one another in plan view (Fig. 5). One of these (Karignan Conglomerate; Figs 2 and 5C) shows a convergence between two coeval bodies in the study area. Internally, FA A is dominated by cross-bedding, with lesser amounts of flat and undular stratification (Table 1, Fig. 4). Largescale (macroform) cross-sets up to 20 m thick were noted in some exposures (for example, Fig. 4A). Dip directions of mesoform cross-bedding preserved within these macroform crosssets are typically 60 to 120 degrees divergent from the macroform dip direction (for example, Fig. 4B). In situ tree fossils were found in a few Permian examples.

Facies Association A — Interpretation

Facies Association A bodies are interpreted as the gravel-dominated fills of sinuous channels on a lowland alluvial plain. The scale of macroform cross-sets suggests that these channels ranged up to 20 m deep. Macroform cross-beds are interpreted as lateral accretion sets, given the angular relationship between macroform and mesoform cross-bed dip directions noted above. Such large-scale cross-strata are interpreted to record systematic meandering behaviour (or, less likely, lateral accretion on mid-channel bars) in large, deep rivers. A sinuous planform is also supported by the mapped plan shape of some bodies (Fig. 5). The convergence noted in the

Table 1. List of facies associations found in the Permo-Triassic Boundary (PTB) interval of the Sydney Basin and their characteristics.

Geometry	Lenticular in cross-section, compensationally stacked, single and multistorey bodies <50 m thick, ribbon-like in planform with lateral pinchout margins. Slight upward convexity to macroform foresets	Lenticular in cross-section, compensationally stacked, single and multistorey bodies <10 m thick, ribbon-like in planform, pinchout lateral boundaries	Multistorey bodies <10 m thick, plan geometry unverified	Wedge-shaped in cross-section, located on the lateral margins of Facies A, B, and C bodies
Sedimentary structures	Crude flat stratification, dune-scale cross-bedding, macroform cross-beds up to 17 m thick, local antidunal stratification, clast imbrication, injection features and soft-sediment deformation structures, <i>in situ</i> fossil tree stumps, wood adpressions and petrified logs. Sandstone partings preserve ripple cross-lamination, planar stratification and coaly traces. No bioturbation, BI = 0	Trough cross-bedding, planar lamination, local internal erosional surfaces, antidunal stratification, injection features and soft-sediment deformation structures, <i>in situ</i> tree stumps, wood adpressions and petrified wood, finely disseminated plant debris and coaly traces. No bioturbation, BI = 0	Trough cross-bedding, rhythmic lamination, planar stratification, ripple cross-lamination, low-angle lamination, lenticular bedding, syneresis cracks, load casts, local root penetration, coaly traces and bioturbation at tops of bodies; BI = 0-2, trace fossil assemblages includes fugichnia, navichnia, <i>Piplocraterion, Rosselia, Teichichnus, Planolites, Thalassinoides, Lockeia</i> and Zoophycos	Ripple cross-lamination and climbing ripple cross-lamination, sinusoidal ripples, flat lamination, minor small-scale cross-bedding, soft-sediment deformation, mudstone clasts, plant debris and coaly traces
Lithology	Poorly to moderately sorted, matrix and clast-supported, locally erosionally based, pebble to cobble conglomerate bodies <50 m thick; matrix is coarse to very coarse-grained sandstone, clasts are various basement types (jasper, quartzite, metsedimentary and volcanic), first cycle pyroclastics, intraformational siltstones and peat rafts. Discontinuous (<3 m thick) medium to very coarse-grained sandstone and mudrock partings	Sharply based bodies of medium to coarse-grained sandstone and pebbly sandstone <pre><10 m thick with lenses of extraformational gravel and intraformational siltstone clast breccia/conglomerate, local mudrock partings</pre>	Erosionally-based bodies of fine to medium-grained sandstone <10 m thick; fine-grained partings with rhythmically interlaminated siltstone-sandstone couplets	Thinly and rhythmically interbedded siltstone and very fine to fine-grained sandstone, intervals <4 m thick
Interpretation	Gravelly alluvial channel fills	Sandy alluvial channel fills	Tidally influenced coastal plain channel fills	Levée
Facies Association	∢	ш	U	Q

(continued)
1.
le
Tab

Facies Association	Interpretation	Lithology	Sedimentary structures	Geometry
ы	Floodbasin deposits on a lowland alluvial plain	Heterolithic (interlaminated and thinly interbedded) very fine to medium-grained sandstone and drab grey (Permian) to greenish grey (Triassic) siltstone, intervals <20 m thick, local sharp-bounded sandstone beds < 0.5 m thick	Ripple cross-lamination, trough cross-bedding, flat lamination, load casts, siderite nodules, common pedogenic modification: slickensides, local red mottling, root penetration, Vertebraria casts, wood adpressions and disseminated plant debris	Sheet-like bodies lateral to Facies A and B. Highly variable thickness but up to 18 m at channel boundaries. Bodies encase and vertically separate Facies A and B bodies
Ŀı	Brackish- influenced coastal plain floodbasin deposits	Heterolithic (interlaminated and thinly-interbedded) very fine to medium-grained sandstone and drab grey (Permian) to greenish grey (Triassic) siltstone, intervals generally <20 m thick, local sharp-bounded sandstone beds <0.5 m thick	Trough cross-bedding, ripple cross- lamination, flat lamination, rhythmic lamination, synaeresis cracks, root penetration, siderite nodules, disseminated plant debris, load casts, BI = 0–2, trace fossil assemblages include fugichnia, navichnia, Teichichnus, Planolites and Reniformichnus australis (McLoughlin et al., in press)	Lateral extent unverifiable. Vertically separates facies C bodies
U	Lacustrine	Dark-light grey shale and siltstone with local interlaminated, very fine-grained sandstone, intervals <2 m thick, principally above uppermost coal seam	Finely laminated, sparse root penetration, macerated plant debris and locally well-preserved leaves of the <i>Glossopteris</i> flora (Permian) and <i>Lepidopteris</i> flora (latest Permian-Triassic), minor and local coal/tuff microbreccia. No bioturbation, BI = 0	Spatially limited and only preserved in sections not affected by fluvial downcutting above uppermost coal seam
Н	Mire	Coal and carbonaceous shale (Permian) in units 2 to 8 m thick, thicker intervals commonly with clastic and pyroclastic partings, local beds of organic-rich microbreccia	Compositional banding and stratification, some intervals massive, coalified plant debris. No bioturbation, ${\rm BI}=0$	Sheet-like over several kilometres. Coal seams split around Facies A, B and C bodies
ы	Pyroclastic fall and flow deposits	Tuff and tuffaceous sandstone, tuff clast sedimentary breccia, intervals <15 m thick	Massive to stratified (flat and undular stratification, local cross-bedding and ripple cross-lamination), some graded beds, soft-sediment deformation, plant roots, fossil tree stumps, leaf fragments, coaly debris and petrified logs	Variable geometries including channel fills. Some bodies are sheet-like, whereas others thicken and thin laterally; local evidence of pinchout

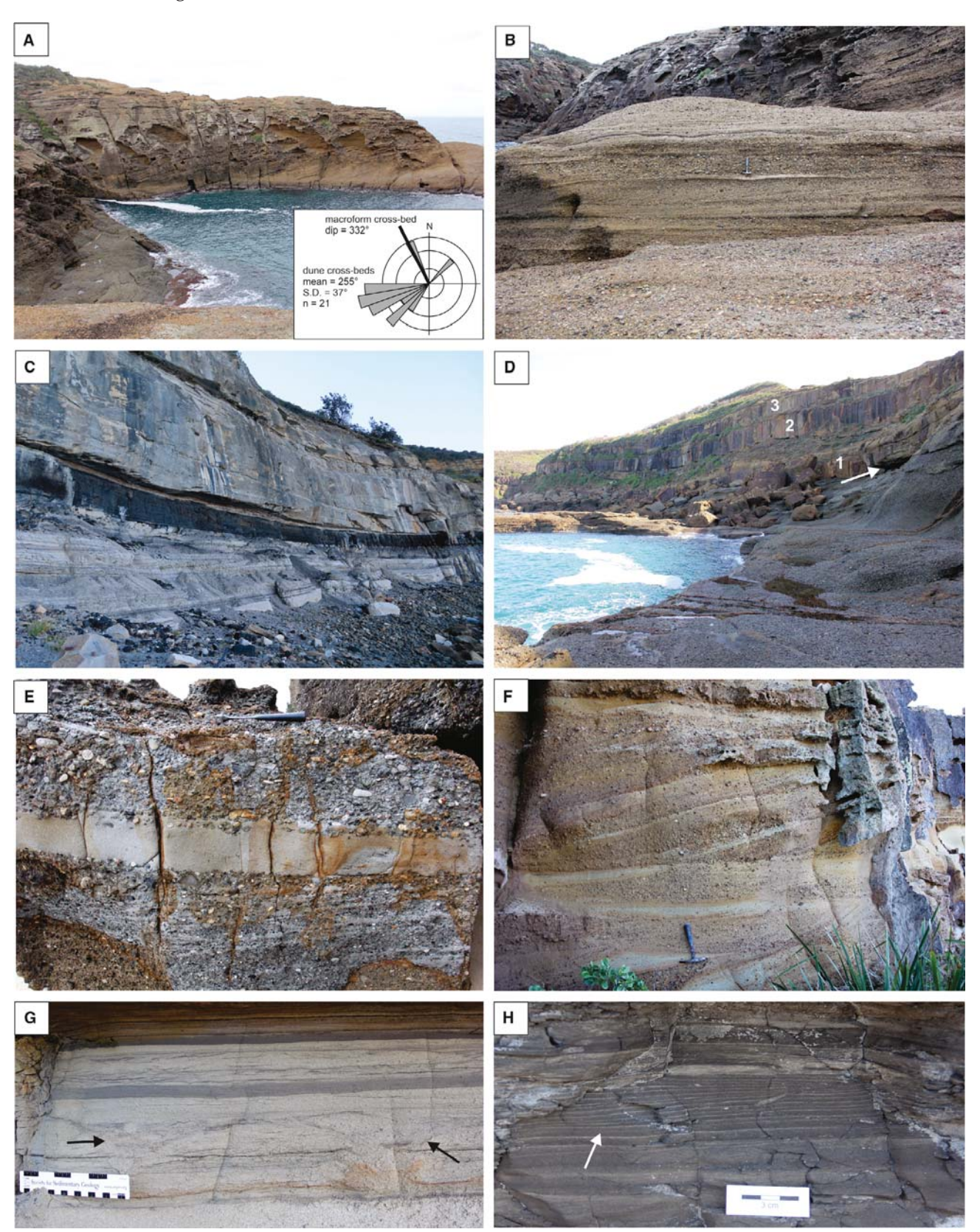


Fig. 4. (A) Upper Teralba Conglomerate exposed at Shark Hole north of Catherine Hill Bay (Newcastle Coalfield) looking north-east, showing a macroform (epsilon) cross-bed at least 17 m thick with rollover and overlying topset, in Facies Association A conglomerates and gravelly sandstones. Inset shows macroform dip direction (bold black line) and palaeoflow directions as indicated by mesoform cross-bedding. (B) Detail of macroform cross-set shown in part (A) (strike view) showing dune-scale cross-bedding oriented at a high angle to the macroform dip direction. This relationship indicates that the macroform cross-set represents lateral accretion in a large, deep fluvial channel. Hammer 0.25 m for scale. (C) View of the Permo-Triassic boundary section at Coalcliff (Illawarra Coalfield), showing the topmost Bulli coal seam, and coastal fluvial channel deposits (Facies Association C) below (Loddon Sandstone Member) and above (Coalcliff Sandstone) the coal. There is little difference in grain size, sedimentary structures, or dispersal direction between the two bodies. Around 20 m of vertical section is shown. (D) View of the Permo-Triassic boundary section on the south side of Wybung Head (Newcastle Coalfield). The uppermost Permian Karignan Conglomerate (Facies Association A) is exposed from sea-level up to the dark overhang where the topmost coal (Vales Point seam) crops out (white arrow). This is in turn overlain by a succession of sharp-bounded gravelly sandstone channel bodies (Facies B and C; cliff-forming units, numbered as in Fig. 12) with intervening coastal floodbasin deposits (Facies Association E; recessive intervals). Approximately 50 m of vertical section is exposed. (E) Close-up view of stratification styles in upper Permian Facies Association A conglomerate and sandstone, Belmont Conglomerate at Stinky Point north of Catherine Hill Bay. Note the different expressions of cross-bedding. Hammer 0.25 m for scale. (F) Close-up view of stratification styles in lowermost Triassic Facies Association A conglomerate and pebbly sandstone, Munmorah Conglomerate at Ghosties Beach. Note the sigmoidal cross-set geometry. Hammer 0.25 m for scale. (G) Detail of stratification style in basal Triassic coastal fluvial channel deposits (Facies Association C), Munmorah Conglomerate, north Birdie Beach. Note ripple cross-laminated sandstone with flaser bedding, disrupted by bioturbation (black arrows) and rhythmic pinstripe lamination (upper half). Scale card 0.15 m. (H) Detail of rhythmic pinstripe lamination (white arrow) in uppermost Permian Loddon Sandstone Member (Facies Association C), Coalcliff.

Karignan Conglomerate (Fig. 5C) is interpreted as a channel confluence, suggesting that channels were, at least in some cases, tributary in nature. The presence of upper flow regime structures and *in situ* tree fossils (Fig. 7) in addition to common cross-bedding suggests that the formative channels experienced a degree of discharge variability, which may have been strongly seasonal (cf. Fielding *et al.*, 2018). The offset stacking pattern of successive channel bodies evident from Fig. 5 is interpreted as a compensational stacking arrangement typical of many alluvial successions (Brown, 1979).

Facies Association B — Description

Facies Association B (FA B) comprises bodies of sandstone with subordinate pebbly sandstone, similar in geometry and internal structure to those of FA A, with which they are closely associated (Table 1, Fig. 6). Mudrock partings are somewhat more abundantly preserved in this FA than in FA A (Fig. 4C). FA B is more widely distributed across the basin than FA A, being the dominant coarse-grained facies away from the axial foredeep of the Newcastle Coalfield. There, sandstone bodies are mosaics of lenses, sheets and channel fills with discontinuous mudrock partings. Macroform cross-beds are

rarely developed, as are upright, in situ tree stumps.

Facies Association B — Interpretation

Facies Association B is interpreted as the fills of sand-bed rivers of similar style to those that formed FA A. In the Newcastle Coalfield, the alternation of storeys of FA A and FA B within composite channel bodies (for example, Fig. 6) suggests that there were periodic pulses of gravel and then sand delivery into the basin, presumably from the rising New England Orogen to the east (Fig. 3). No significant differences were noted in palaeoflow distributions between FA A and FA B in this area, suggesting that provenance was consistent. This in turn suggests that there were pulses of orogenic uplift that periodically delivered quantities of gravel into the basin. This is similar to the pattern established in the eastern Bowen Basin in Queensland during the late Permian and Early Triassic (Holcombe et al., 1997; Fielding et al., 1997), where several wedges of orogen-derived conglomerate are interpreted to record orogenic pulses. Elsewhere in the basin, FA B accounts for entire channel bodies. Their internal architecture suggests that formative rivers were mobile, sand-bed streams of varying planform. As with FA A, preservation of upright, in situ tree

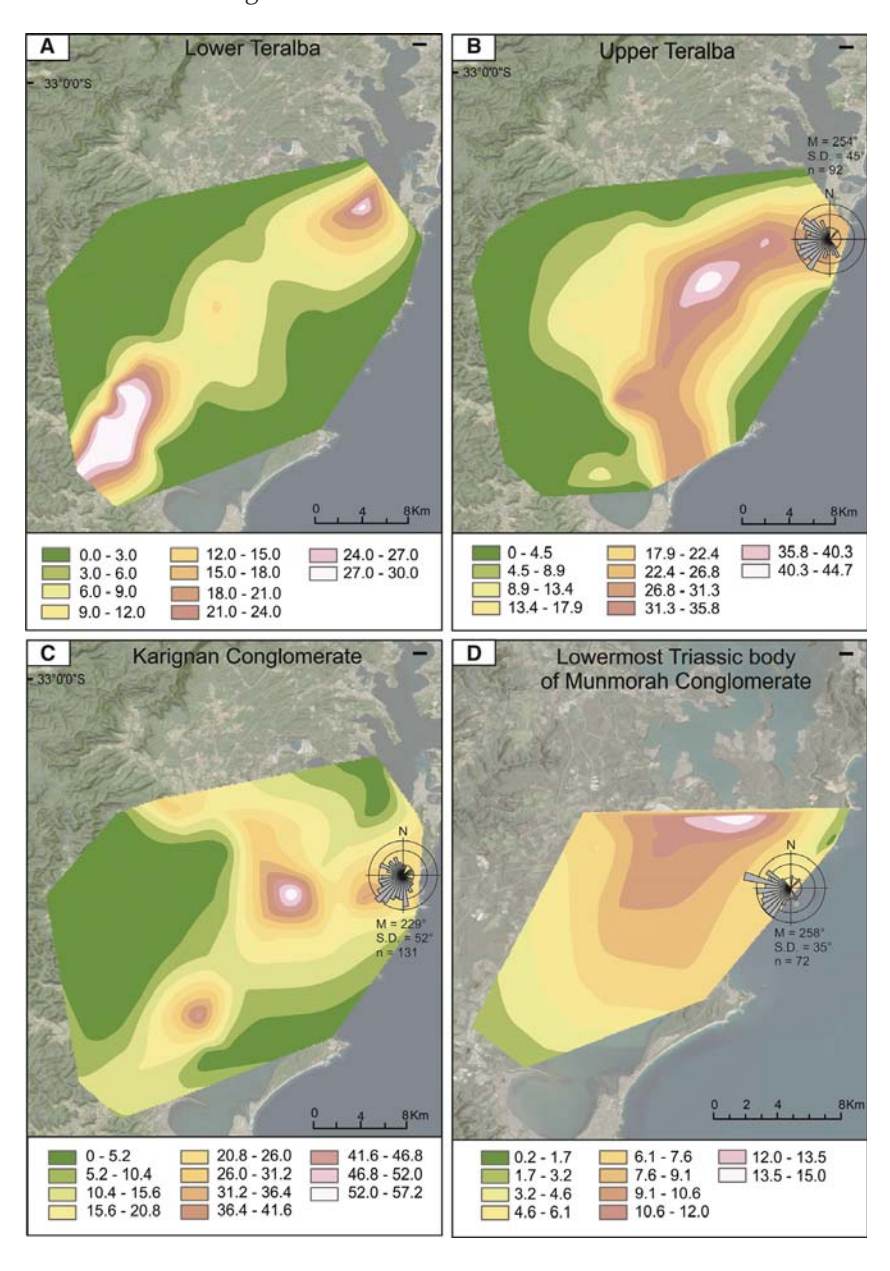


Fig. 5. Maps showing the plan geometry of four successive channel bodies within the uppermost Permian and lowermost Triassic succession of the Newcastle Coalfield: in ascending stratigraphic order, (A) lower Teralba Conglomerate, (B) upper Teralba Conglomerate, (C) Karignan Conglomerate, and (D) lowermost Munmorah Conglomerate (see Fig. 6 for stratigraphic context). Note the south-westerly linear trend to these bodies, consistent with palaeoflow data from coastal surface exposures. Note also the offset (compensational) stacking pattern to successive bodies, and the preservation of a channel belt confluence with a confluence scour fill in the Karignan Conglomerate.

stumps (only within the Permian succession) and upper flow regime structures suggests a strongly seasonal discharge regime at times.

Facies Association C — Description

Facies Association C (FA C) comprises sandstone and gravelly sandstone bodies similar to FA B, but with some features unique to this FA. Principal among these are taxonomically restricted trace fossil assemblages, particularly in heterolithic partings (Table 1, Fig. 4G), synaeresis cracks and rhythmically laminated heterolithic partings (Fig. 4G and H). Mudrock partings are more abundant than in FA B, and palaeoflow distributions from cross-bedding and other sedimentary structures are in some cases bimodal to multimodal.

Facies Association C — Interpretation

Facies Association C is interpreted as the deposits of coastal plain alluvial channels affected to varying extents by tidal backflow and inundation by brackish water. Bimodal (often bipolar) palaeoflow distributions attest to the role of tidal backflow, and rhythmically laminated heteroliths are strongly similar to tidal rhythmites formed in the tidal reaches of coastal rivers (cf. Dalrymple & Choi, 2007; Martinius & Berg, 2011). Trace fossil

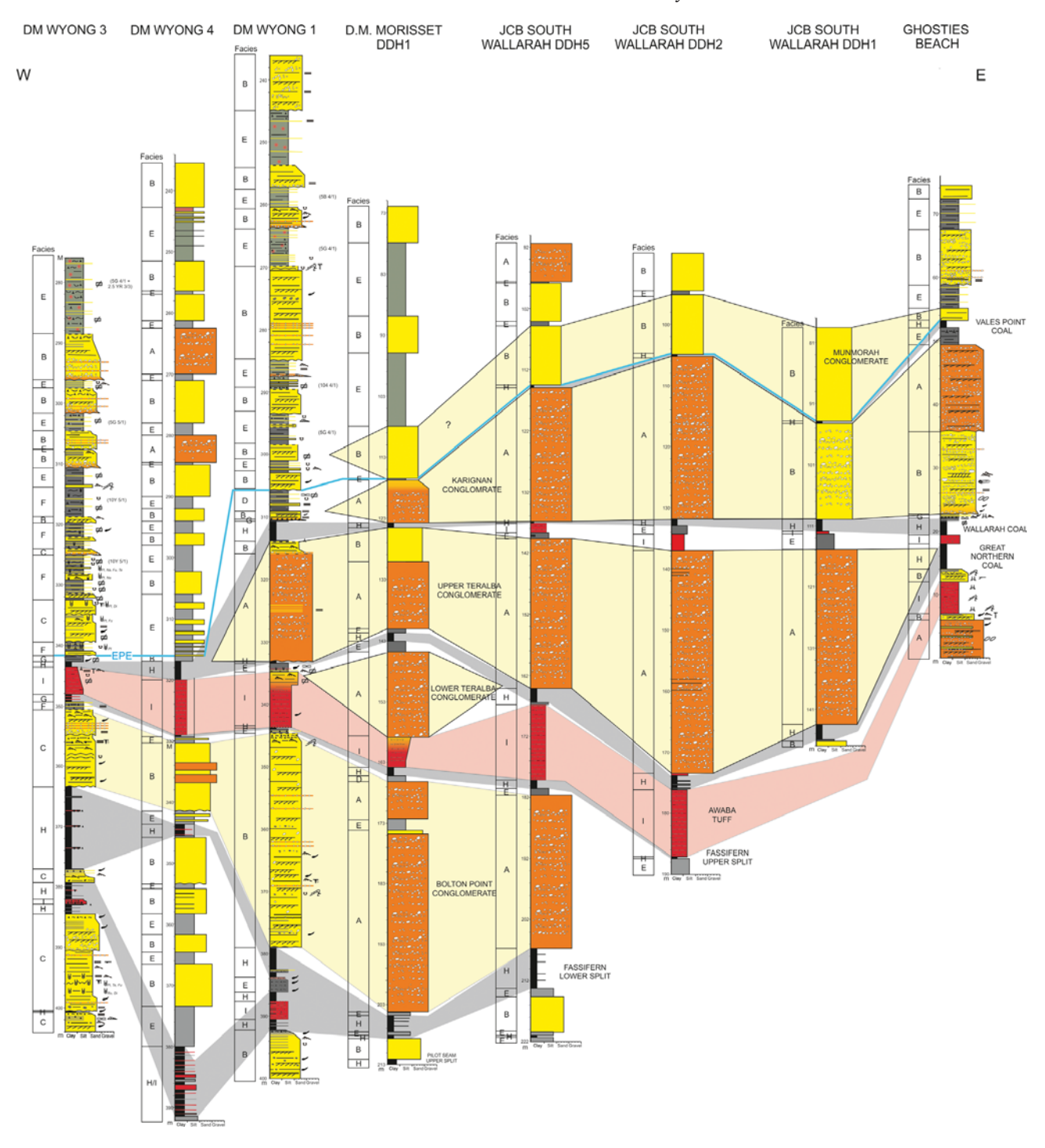


Fig. 6. West—east cross-section across part of the Newcastle Coalfield (see Fig. 1 for location) to show stacking patterns of sediment bodies in the late Permian and earliest Triassic succession. Note the confinement of some conglomeratic channel fill bodies (Facies Association A) within coal seam splits, the complex lateral interfingering between conglomerate (Facies Association A) and sandstone (Facies Association B) channel bodies, and the extensive nature of tuff beds (Facies Association I) that can, therefore, be used as regional stratigraphic markers. The EPE horizon is shown as a blue line. See Fig. 1 for line of section and Fig. 12 for key to symbols and lithology colours used.

assemblages are typical of those found in tidal fluvial settings (Gingras & MacEachern, 2012). Similar trace assemblages were documented by Fielding (2015) from coeval coastal alluvial and estuarine strata of the Rangal Coal Measures from the Bowen Basin in Queensland.

Facies Association D — Description

Facies Association D (FA D) comprises rhythmically interbedded sandstone and siltstone on a decimetre scale, in intervals up to a few metres in thickness (Table 1), commonly occurring as component storeys of multistorey sandstone channel (FA B) bodies (Fig. 8A). In cross-section these bodies are laterally discontinuous wedges, showing lateral pinchout or erosional truncation beneath overlying sandstones (Fig. 8A). Various mainly ripple-scale sedimentary structures are present, and plant fossils are abundantly preserved on bedding planes (including delicate leaves of the sphenopsid *Schizoneura gondwanensis* in the uppermost Changhsingian to basal Triassic Coalcliff Sandstone).

Facies Association D — Interpretation

The distinctive, rhythmically interbedded lithology and context of FA D (Fig. 8A) suggests its origin as levée deposits associated with sandy alluvial channels (e.g. Fielding, 1986; Fielding et al., 1993; Brierley et al., 1997; Adams et al., 2004; Filguera-Rivera et al., 2007). Sedimentary structures indicate rapid sediment fallout from decelerating currents, presumably overbank flows during high flow stage in adjacent alluvial channels. Preservation of delicate plant fossils suggests that parts, perhaps the crests, of levées were vegetated and that plant debris was buried rapidly during high flow events.

Facies Association E — Description

Facies Association E (FA E) comprises mudrocks and sandstones interlaminated and interbedded on various scales (heteroliths; Fig. 8B and C). Occurrences in the Permian succession are ubiquitously medium to dark grey (Fig. 8C and D), whereas above the Permo-Triassic boundary they take on blue-grey and green-grey hues with red-brown mottling, stronger hues becoming evident upward over tens of metres vertical intervals. Many occurrences are short (<2 m thick) intervals between FA A to FA C channel bodies, but in some locations, such as at Frazer Beach (Fig. 8B), continuous intervals generally <20 m thick are preserved. Some examples show 1 to 5 m thick coarsening-upward sequences (for example, Fig. 8D). In situ plant roots, detrital plant fragments and textural modification of mudrocks (blocky structure and slickensides) are common. Discrete, sharp-bounded sandstone beds are preserved locally (for example, Fig. 8B), and in the Triassic succession preserve local desiccation cracks on bed bases.

Facies Association E - Interpretation

Facies Association E is interpreted as overbank deposits on lowland alluvial floodplains, by analogy with modern and ancient examples worldwide. Drab grey colours indicate that waterlogged conditions prevailed during the Permian,





Fig. 7. Illustrations of features indicative of highly seasonal discharge variability (moderate to high Coefficient of Variance, in the scheme of Fielding *et al.*, 2018) in alluvial channel deposits. (A) Supercritically climbing antidunal stratification preserved in a Facies Association B body, lower Karignan Conglomerate at Ghosties Beach. Hammer (circled) is 0.25 m. Note the train of at least two coeval bedforms (wavelength 4.3 m, height, 0.4 m) migrating right to left, consistent with the dip orientation of cross-bedding in the underlying bed (arrowed). (B) Upright, *in situ* tree fossil in the Facies Association B channel sandstone, base of lower Karignan Conglomerate at Ghosties Beach. The tree (to left of scale) was rooted into the siltstone underlying the erosionally-based sandstone, but it was clearly extant during channel sedimentation. Scale card 0.15 m.



Fig. 8. Illustrations of Facies Associations D to G. (A) View of the Bulli Coal (FA H) overlain by the Coalcliff Sandstone at Coalcliff, with two intervals of FA D (levée deposits) interbedded with sandstone bodies representing FAs B and C (channel deposits). Total ca 10 m of vertical section visible. Facies Associations (Table 1) are annotated on the left side of the image. (B) View of the Vales Point Coal (FA H) overlain by the Dooralong Shale (FAs G and E) and then Munmorah conglomerate (FA B) at Frazer Beach. Total ca 30 m of vertical section shown. Facies Associations (Table 1) are annotated on the left side of the image. (C) Close-up image of the boundary interval in PHK Eveleigh-1. Top of the Bulli Coal (removed for destructive analysis) is shown on the bottom left. Directly overlying this is a dark, laminated fine-grained siltstone (FA G), which passes up into medium grey siltstones with sand laminae (FA E), in turn erosionally truncated by an FA B sandstone. Core is 55 mm in diameter. (D) Close-up image of the boundary interval in EHK Lisarow-1. Top of the Vales Point Coal (removed for destructive analysis) is shown on the lower left. Directly overlying this is a dark, laminated, fine-grained siltstone (FA G), which passes upward into medium grey siltstones with increasing interlaminated and interbedded sandstone upward (FA E). This coarsening-upward interval shows soft-sediment deformation and indeterminate bioturbation (white arrows). Scale is 50 mm. (E) Close-up view of bioturbated (white arrows), interlaminated siltstone and sandstone (FA F) from DM Wyong-3, above the Vales Point Coal. Scale card is 30 mm.

becoming more frequently or seasonally drained and exposed upward into the basal Triassic section. Colouration, textural modification and in situ plant roots all indicate pedogenic modification of the alluvial surface, and the drab colours, together with a lack of horizonation, suggest that substrates were predominantly waterlogged (gleyed; Duchaufour, 1982; Besly & Fielding, 1989; Tabor et al., 2017). Increasingly strong hues upward over an interval of 5 to 25 m indicate greater and more frequent levels of exposure and oxidation, consistent with the preservation of desiccation cracks at some levels. Sharpbounded sandstone beds are interpreted as deposits of splays and splay complexes, formed by overbank flooding during high flow stage in nearby river channels (cf. Bridge, 1984; Jorgensen & Fielding, 1996; Ethridge et al., 1999; Burns et al., 2019). Short coarsening-upward sequences are analogous to crevasse-derived minor deltas reported from modern and ancient alluvial and coastal plain settings (Elliott, 1974; Fielding, 1984; Tye & Coleman, 1989; Perez-Arlucea & Smith, 1999; Farrell, 2001).

Facies Association F — Description

Facies Association F (FA F) entails similar lithologies and vertical successions to FA E but, additionally, preserves suites of bioturbation, rhythmic lamination and common synaeresis cracks (for example, Fig. 8D and E; Table 1). Bioturbation intensities are typically low, as are the taxonomic diversities of trace fossils (typically between one and three taxa, locally less than six taxa). In the Frazer Beach - Wybung Head area (Fig. 1), a monogeneric suite of large, ovoid burrows was found subtending from the base of a tabular sandstone bed, flattening out downward through dark grey shales of FA G into the top of the underlying Vales Point Coal, i.e. penetrating the EPE horizon (McLoughlin et al., in press).

Facies Association F — Interpretation

The broad interpretation of FA F is similar to that for FA E, i.e. low-lying floodplain and floodbasin deposits, but with the distinction that FA F preserves characteristics of coastal settings, in the form of subaqueous shrinkage (synaeresis) cracks and low-diversity trace fossil suites that are commonly associated with brackish water settings (MacEachern & Gingras, 2007; Gingras

et al., 2011; Gingras & MacEachern, 2012). Coarsening-upward cycles (for example, Fig. 8D) in this context may record infilling of open bays in a lower, tidally influenced coastal plain. The large burrows initiating above the terrestrial extinction horizon at Frazer Beach (Vajda et al., 2020) have been referred to Reniformichnus australis by McLoughlin et al. (in press) and attributed to the activity of small, fossorial cynodonts.

Facies Association G — Description

Facies Association G (FA G) comprises thin intervals of dark grey, thinly laminated (fissile) mudrocks. One particularly persistent occurrence of this facies directly overlies the uppermost coal seam in the Permian succession (Fig. 8C and D), from which palynological samples yielded only degraded wood debris, charcoal fragments and fungal remains (Vajda *et al.*, 2020).

Facies Association G — Interpretation

Facies Association G is interpreted as the deposits of shallow lakes and ponds on the coastal alluvial plain, by association with enclosing facies. The lack of bioturbation and fissile character of the mudrocks argues for a dysoxic to anoxic lake bottom environment. Eutrophic conditions are indicated by the lithology, geochemistry and palynological assemblage (Vajda *et al.*, 2020). The notable occurrence directly above the uppermost Permian coal seam is interpreted to record the end-Permian plant extinction event (Fielding *et al.*, 2019; Vajda *et al.*, 2020). This is the manifestation of the 'dead zone' of Vajda *et al.* (2020).

Facies Association H — Description

Facies Association H (FA H) consists of seams of black coal and coaly shale up to 8 m thick, many of which are composite (Fig. 9A and B; Table 1). Coals are mainly composed of bright banded lithotypes but are both laterally and vertically variable. Coal seams show a propensity to split dichotomously into the margins of channel bodies (FAs A to C; for example, Fig. 6). Partings of siliciclastic and pyroclastic lithologies are common (Fig. 9A). Included among these partings are discontinuous beds of organic-rich microbreccia <0.1 m thick (Fig. 9C to F). These lithologies comprise massive to crudely stratified admixtures of silt-size mineral grains, organic debris, and irregularly shaped

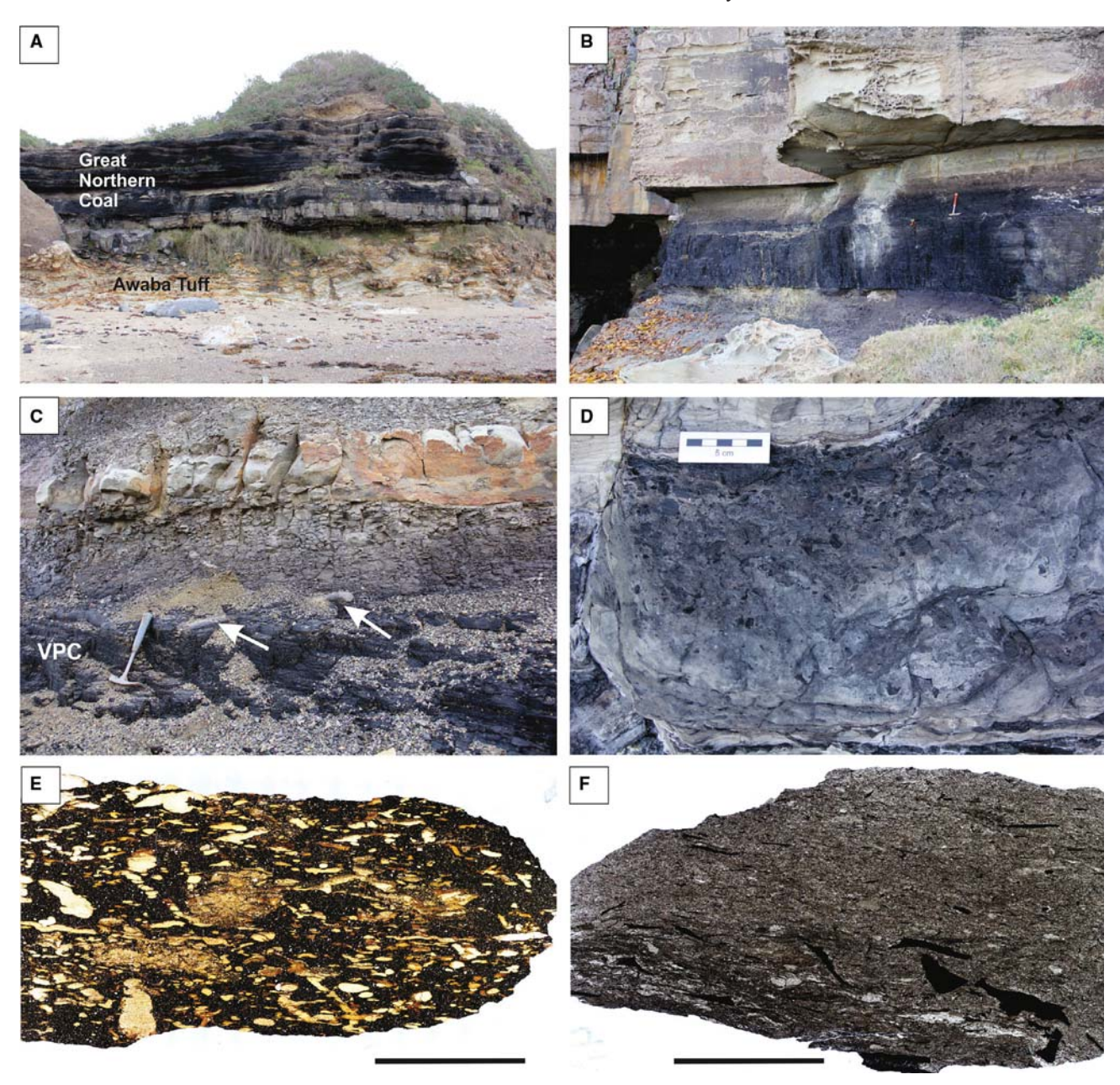


Fig. 9. Illustrations of Facies Associations H and I. (A) Outcrop view of the Awaba Tuff (FA I) overlain by the Great Northern Coal FA H) at Spoon Rocks. Note the pervasive soft-sediment deformation in the tuff and the strongly interbedded character of the coal. Total ca 10 m of vertical section visible. (B) Outcrop view of the Vales Point Coal (FA H) south of Wybung Head. The coal is overlain by weathered mudrocks of FAs E and G, in turn erosionally truncated by a sandstone body of FA B. Hammer is 300 mm long. (C) View of the Vales Point Coal (VPC) at Frazer Beach, with the organic-rich microbreccia bed at the top and overlying lacustrine shale (FA G), passing up into poorly-drained floodplain deposits (FA F) with a sharp-bounded sandstone bed of interpreted splay origin. Note the large, obliquely inclined, tubular burrows that subtend from the base of this bed (Reniformichnus australis of McLoughlin et al., in press; white arrows). Hammer 0.25 m for scale. (D) Close-up view of organic-rich microbreccia in the top of the Wallarah Coal at Ghosties Beach. Note the admixture of plant-derived organic debris (dark grey to black particles) including charcoal in a mixed clastic matrix. Scale card 5 cm. (E) Thin-section scan of the organic-rich microbreccia from the top of the Vales Point Coal at Frazer Beach, showing the admixture of fine organic debris (black), mineral grains (white) and probable volcanic pumice fragments (light brown). This is the bed figured by Retallack (2005, fig. 4B). Plane-polarized light. Scale bar 1 cm. (F) Thin-section scan of the organic-rich microbreccia from the top of the Wallarah Coal at Ghosties Beach, showing an abundance of macroscopic organic fragments (black), mineral grains (white) and less abundant, probable volcanic pumice fragments (grey to light brown). Plane-polarized light. Scale bar 1 cm.

clasts up to small pebble size of probable volcanic pumice in varying abundances (Fig. 9C to F). They occur at various levels in the Permian succession including at the top of the Vales Point Coal in the Munmorah area where they were documented by Retallack (2005). Rare nodules of silicified and calcified peat from Wuchiapingian coal seams in the southern part of the basin entomb three-dimensionally preserved mire plants dominated by the remains of glossopterid woody gymnosperms, but also including a range of herbaceous ferns and lycopsids, and fungi (Pigg & McLoughlin, 1997; McLoughlin et al., 2019).

Facies Association H — Interpretation

Coal seams represent fossilized bodies of peat, formed in coastal plain mires where the Glossopteris flora thrived. Fluctuations in the palaeowater table gave rise to the variability in lithotypes, as is typical of bituminous rank coals in general. The mostly simple seam splits are attributed to a combination of differential compaction of peat-rich substrates and the introduction of channel sediments into parts of mires, leading to the avulsion of channels to new courses (Fig. 5). Organic-rich microbreccias are interpreted to record floods of eroded debris that were redeposited in shallow standing water within mire settings. The occurrence of such facies at several levels within the Permian succession suggests that they were not the product of catastrophic landscape degradation only at the Permo-Triassic boundary, as was suggested by Retallack (2005). Rather, they seem to record a process of local erosion and redeposition that was intermittent but not exceptional. Given the variable content of what appears to be volcanic fallout (Fig. 9E and

F), the trigger for these events may have been ash showers from distant volcanic eruptions. Texturally similar microbreccias have been interpreted as having a partly pyroclastic provenance both in this succession (e.g. fig. 2 of Diessel & Moelle, 1965; fig. 6.37 of Diessel, 1992) and in others (e.g. fig. 4 of Jorgensen & Fielding, 1999; fig. 7F of Yago & Fielding, 2015).

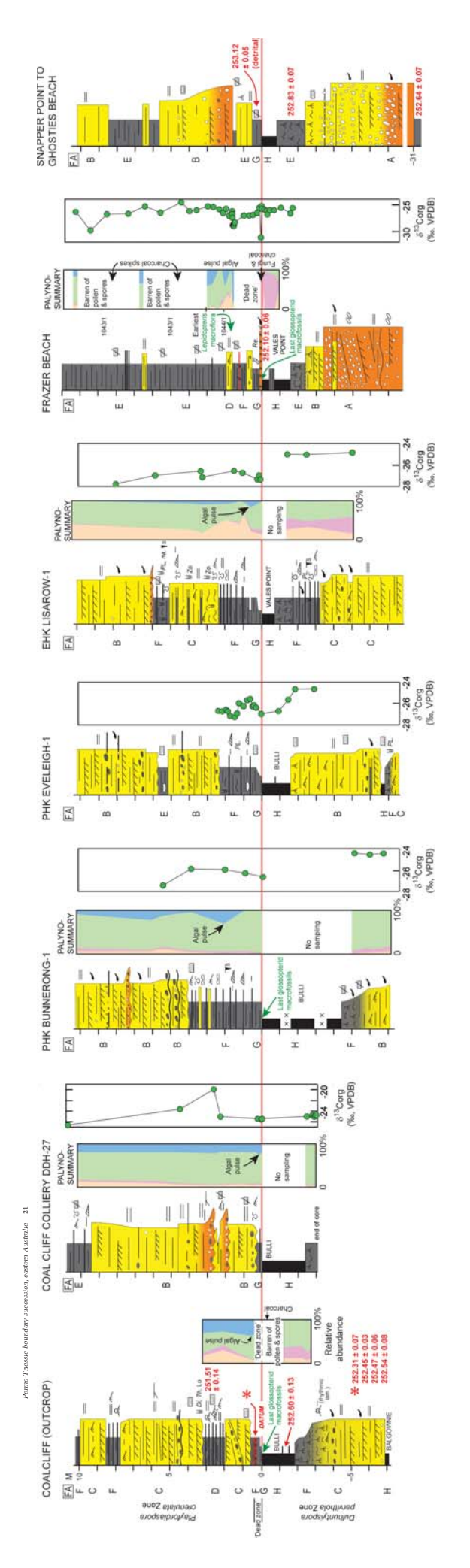
Facies Association I – Description

Facies Association I (FA I) comprises bodies of cream-coloured tuff, tuffaceous sandstone and tuffaceous siltstone <15 m thick that have a pronounced soapy texture and preserve various physical sedimentary structures and plant fossils (Table 1). Locally, this lithology grades into monomictic sedimentary breccia comprising principally tuffaceous clasts in a mixed siliciclastic–tuffaceous matrix and overlying pronounced erosion surfaces. Many beds preserve spectacular permineralized logs and *in situ* tree stumps. Indeed, at Reids Mistake near Swansea, horizontal fossil tree trunks are aligned in the same direction as tilted, *in situ* stumps (towards the west; David, 1907; Diessel, 1992).

Facies Association I – Interpretation

Facies Association I is interpreted as the deposits of pyroclastic airfall, and locally pyroclastic surge and flow deposits. Arrays of prostrate fossil tree trunks at Reids Mistake all aligned to the west suggest that fossil lowland forests were at times destroyed by high-velocity lateral blasts from stratovolcanoes located to the east (David, 1907; Diessel, 1992). Some volcanic sources were evidently located no more than a few tens of kilometres from the outcrop belt (given the

Fig. 10. Cross-section showing facies relationships across the end-Permian Extinction Event (EPE) and Permo-Triassic Boundary (PTB) from the southern Sydney Basin (Coalcliff), through the synclinal axis (PHK Bunnerong-1, PHK Eveleigh-1) to the northern Sydney Basin (EHK Lisarow-1, Frazer Beach, Snapper Point to Ghosties Beach). Above the uppermost coal seam is a persistent interval of fine-grained, lacustrine mudrock (Facies Association G; Table 1) in which the floral extirpation is recorded. Geochronological data indicate this event occurred 252.54 ± 0.08 to 252.10 ± 0.06 Ma. This Dead Zone grades upward into floodbasin deposits (Facies Associations E and F) and typically then into erosionally based channel sandstones (Facies Associations B and C). A new age from the Coalcliff Sandstone suggests that the PTB is at the base of the first erosionally based channel body above the uppermost coal and the Dead Zone. Mudrocks are grey colours unless otherwise noted by Munsell codes. Palynosummary categories (left to right): non-taeniate bisaccate pollen (yellow), taeniate bisaccate pollen (pink), plant spores (green) and algae/acritarchs (blue). 'Dead zone' defined by the interval between the last occurrence of glossopterid macrofloral remains, and the first appearance of *Playfordiaspora crenulata* Zone spore-pollen index taxa. Age data from Metcalfe *et al.* (2015), Fielding *et al.* (2019) and new data reported herein (see Data S1). Frazer Beach palynosummary is a composite of data from Frazer Beach and nearby Snapper Point (after Vajda *et al.*, 2020). Also shown are carbon-isotopic profiles. See Fig. 12 for key to symbols and lithology colours used.



to Anthron Suffmantalant D 2000 International Association of Selimantalandes Selimantalan

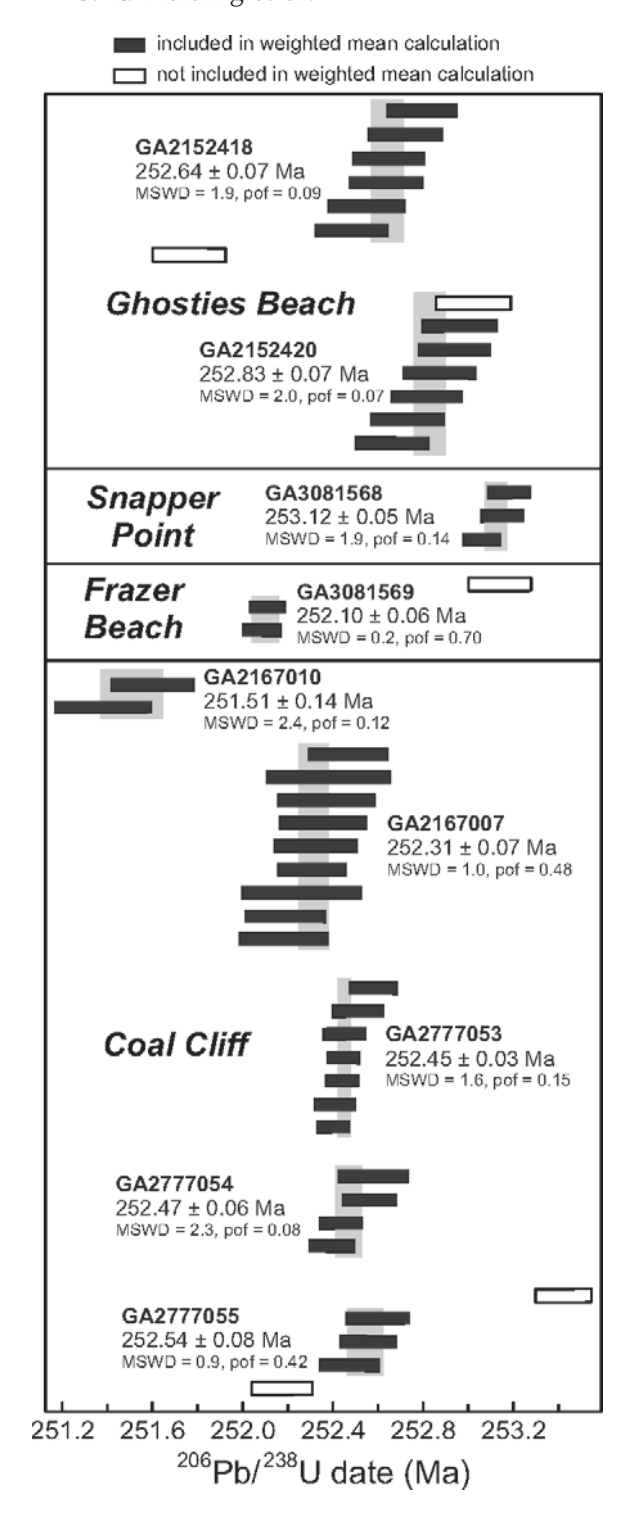
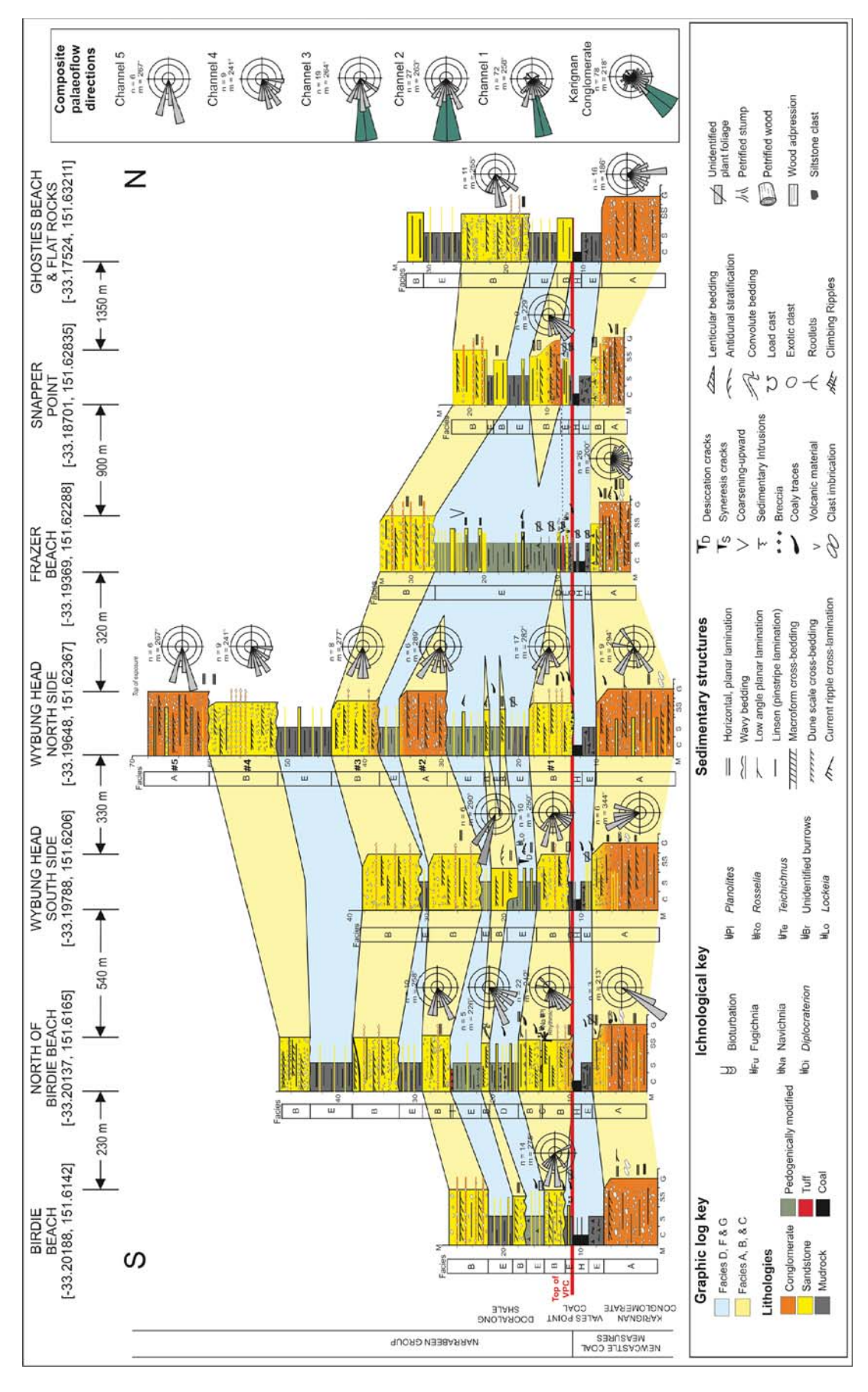


Fig. 11. Ranked date plot showing age spectra with errors for the new ages reported in this paper. See Data S1 for full details of analytical methods and results. Ages are considered as Maximum Depositional Ages owing to the small number of dateable zircon grains and the significant population of detrital zircon in all samples.

preservation of these typically proximal pyroclastic surge and flow facies; Cas & Wright, 1987), whereas others were more distant, given the basinwide distribution of some tuff beds. Other units of FA I comprise thick intervals of airfall tuff that again were probably derived from high-volume, explosive volcanic eruptions in the orogenic hinterland to the east. Such intervals tend to be profoundly soft-sediment-deformed, suggesting that volcanic fallout landed on waterlogged surfaces that were prone to in situ foundering and other forms of surface deformation. Evidence that volcaniclastic sediment at times overwhelmed the natural depositional system is preserved in the form of tuff breccia-filled channels at Reids Mistake and elsewhere. Such phenomena have been recorded from some modern stratovolcano eruptions including those of Mount Pinatubo, Philippines (Newhall & Punongbayan, 1996) and Mount Rainier, western USA (Vallance & Scott, 1997).

IDENTIFICATION OF THE END-PERMIAN EXTINCTION (EPE) AND PERMO-TRIASSIC BOUNDARY (PTB)

The default placement of the Permo-Triassic boundary in the Sydney Basin has to date been the top of the uppermost coal seam (Bulli seam in the south, Katoomba seam in the west, and Vales Point seam in the north-east of the Sydney Basin; Coalfield Geology Council of New South Wales, 1999; Fig. 2). Radiogenic isotopic ages, palynological data and carbon isotope profiles reported by Fielding et al. (2019) from the present study area indicated: (i) that the PTB is somewhat higher than the top of the uppermost coal, most likely in overlying thinly interbedded strata (FA E/FA F) where substantial intervals of such facies are preserved above the coal, or at the base of the first fluvial channel body where these 'roof shales' were later erosionally excised; and (ii) that the continental EPE in the Sydney Basin, as expressed by the palaeofloral turnover, 400 kyr occurred some prior the 251.902 ± 0.024 Ma PTB, and as much as 360 kyr prior to the onset of the marine extinction at 251.941 \pm 0.037 Ma as determined from the GSSP and other locations in China (Burgess et al., 2014). This placement of the terrestrial EPE at high southern latitudes is consistent with recent radiogenic-isotope age constraints on the



Note the compensational stacking pattern of channel bodies above the Vales Point Coal (which is the datum; red line). The line of the cross-section is roughly perpendicular to palaeoflow direction and is shown in Fig. 1. Key to symbols and lithology colours used in all graphic logs is also shown. Fig. 12. Cross-section along the coastal exposures of the Northern Coalfield from Birdie Beach in the south to Ghosties Beach in the north, showing facies relationships across the end-Permian Extinction Event (EPE) and Permo-Triassic Boundary (PTB), channel body correlations and palaeoflow data. Channel bodies 1 to 5 are labelled on the Wybung Head North side log, and overall palaeoflow distributions for each channel body are given to the right of the panel.

vertebrate faunal turnover in the Karoo Basin, South Africa (Gastaldo *et al.*, 2020). Herein, seven additional, new CA-ID-TIMS U-Pb ages are reported that further constrain the timing of the floral extirpation to 252.54 \pm 0.08–252.10 \pm 0.06 Ma (Figs 10 and 11; Data S1). This broadens the range of estimates of the floral extinction event to between 600 and 200 kyr before the PTB and the marine extinction.

Where the topmost coal is not immediately overlain by a fluvial channel sandstone, the Permo-Triassic transition is conformable and relatively complete stratigraphically, as established above and by Fielding et al. (2019). In such cases (Fig. 10), the facies immediately overlying the top coal is typically dark grey, laminated to fissile, organic-rich mudrock (shale; FA G). This facies association corresponds to the post-EPE 'dead zone' (sensu Vajda et al., 2020; Fig. 10). This study reports that the FA G interval at Coalcliff, southern Sydney Basin, expresses an almost identical palynofloral record to that of Frazer Beach (Fig. 10), indicating that this pattern of lacustrine sedimentation and floral impoverishment likely occurred across much of the Sydney Basin. Specifically, the palynological record reveals an interval of high charcoal relative abundances, and low spore-pollen abundances in this short interval. Mudrocks in the immediate roof of the top coal typically coarsen upward over 2 to 5 m into thinly interbedded siltstone and sandstone or thinly bedded fine-grained sandstone of Facies Association F. In some cases, the same interval is composed of interbedded siltstone and tabular, sharp-bounded sandstone beds of Facies Association E. Physical sedimentary structures are dominated by current ripple crosslamination with subordinate wave-generated and combined-flow ripples. Subaqueous shrinkage (synaeresis) cracks are common, as is a taxonomically restricted suite of small, sporadically distributed, facies-crossing trace fossils. In a small subset of cores studied (particularly around Wyong; Fig. 1), the trace fossil suite was somewhat more diverse and included Diplocraterion and other typical facies-crossing traces (Table 1; Gingras et al., 2011). These facies provide the first abundant palynoassemblages above the EPE, and reveal a marked increase in algae and a change from taeniate bisaccate pollen (typical of glossopterids) to non-taeniate bisaccate pollen (typical of conifers and corystosperms). These strata are typically overlain either by channel deposits (FA B and FA C) or by further floodbasin deposits (FA E and FA F).

The laminated mudrocks and short coarsening-upward cycles are interpreted as the deposits of shallow coastal lakes, the water in which was subject to salinity fluctuations. The rare preservation of coastal/marine trace fossils in a few bores in the basin depocentre area around Wyong may indicate that brief marine incursions accessed these more rapidly-subsiding areas. The interbedded mudrocks and tabular sandstones are interpreted to record shallow floodbasin deposits with splays derived from nearby fluvial channel margins. There is no evidence for immediate aridification of the landscape. Indeed, the observation that the most common facies overlying the uppermost coal is representative of deposition under standing water was interpreted by Vaida et al. (2020) as evidence of ponding of surface water following extinction of the lowland Glossopteris flora. Although vegetation productivity was significantly lower until at least the Spathian (ca 248 Ma; Mays et al., 2020), the first elements of a Triassic recovery flora, documented in detail at Frazer Beach (Fielding et al., 2019; Vajda et al., 2020), coincide with a return to fluvial facies (FAs B and C; Table 1, Fig. 10) similar to those of the uppermost Permian. These sandstone bodies are shown in Fig. 12 to interfinger with Facies Association E and F floodbasin deposits. A new CA-ID-TIMS U-Pb age of 251.51 ± 0.14 Ma from a fine-grained parting within the Coalcliff Sandstone at Coalcliff (Fig. 10) suggests that the base of the first fluvial channel body (or its overbank facies equivalent) above the uppermost coal and the Dead Zone, where preserved, likely represents the Permo-Triassic boundary.

FLUVIAL STYLE, CHANNEL BODY GEOMETRY AND SEDIMENT DISPERSAL

Surface data

Insights into the two-dimensional and three-dimensional geometry of channel sediment bodies can be gained both from laterally continuous cliff exposures in both the southern and northern coastal outcrop belts (Fig. 1) and from correlation of subsurface intersections in cored boreholes. The exposures in the Northern (Newcastle) Coalfield around the Munmorah State Recreation Area, are particularly instructive. A cross-section (Fig. 12) was constructed by physical tracing of beds on either side of the

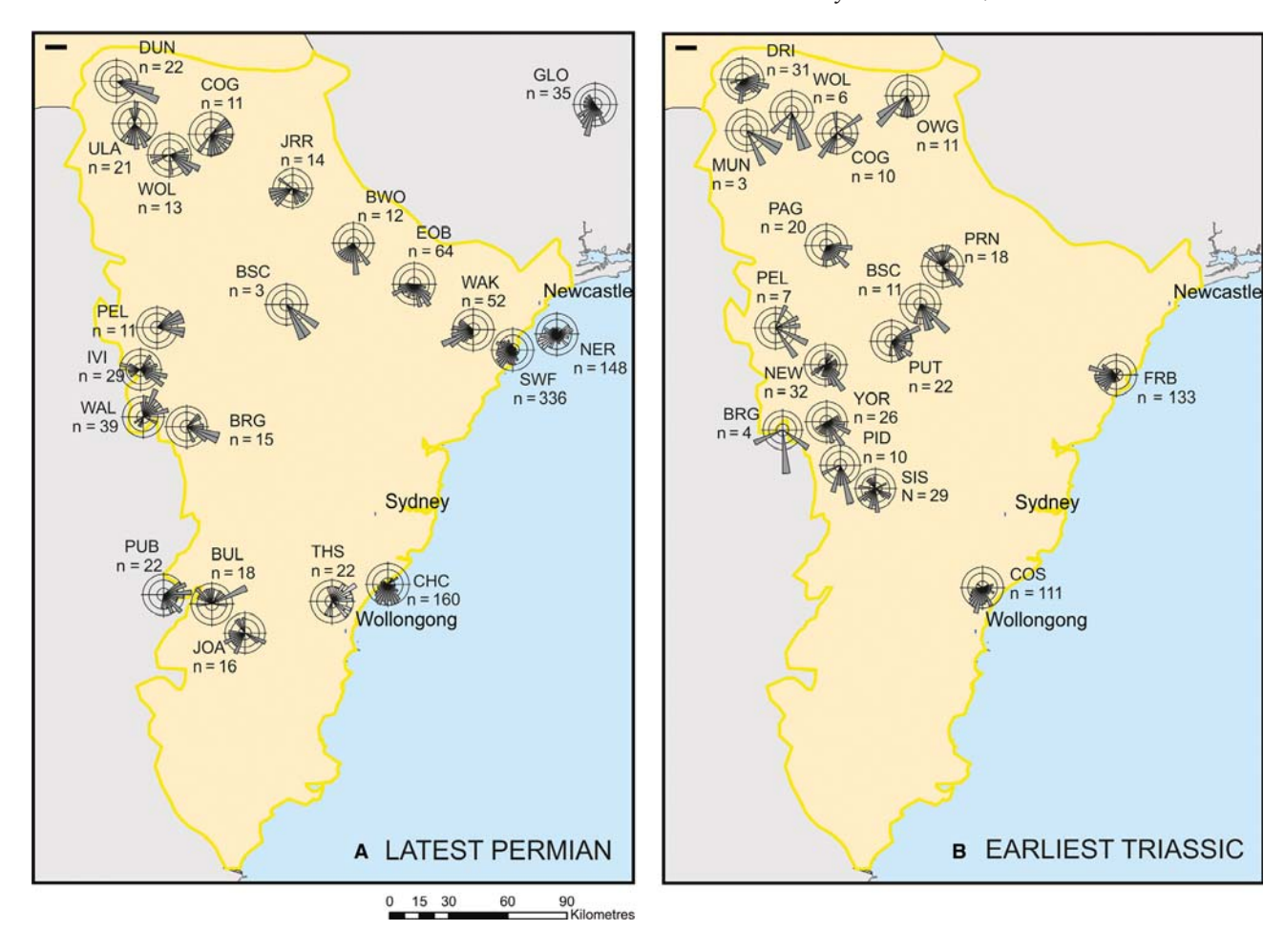


Fig. 13. Maps of the Sydney Basin showing the regional distribution of palaeoflow from channel bodies (Facies Associations A to C) in (A) latest Permian and (B) earliest Triassic strata. Note the generally centripetal palaeoflow pattern into the north–south depocentre between Newcastle and Sydney, and then southward down the basin axis. This pattern does not change substantially across the Permo-Triassic Boundary.

Table 2. Composition of Permo-Triassic sandstones in PHK Bunnerong DDH-1, Sydney Basin, Australia, based on point counting of framework grains in thin section.

Depth (m)	Age	Quartz (%)	Feldspar (%)	Rock fragments (%)	Lithology
723.58	Triassic	15	3	82	Litharenite
767.10	Triassic	19	9	72	Litharenite
799.97	Triassic	11	4	85	Litharenite
953.90	Permian	16	2	82	Litharenite
1171.81	Permian	0	1	99	Litharenite
1198.64	Permian	1	6	93	Litharenite

uppermost coal seam (Vales Point Coal; VPC) from Birdie Beach in the south to Ghosties Beach in the north (Fig. 1). Below the VPC, the succession is dominated by a thick, laterally extensive conglomerate-dominated channel body (FA A), which fines upward abruptly into the VPC. Immediately above the VPC (FA H) is a

short (<1 m) interval of dark grey shales (FA G; Vajda *et al.*, 2020), in turn overlain by a mosaic of discontinuous sandstone and pebbly sandstone channel bodies (FAs B and C) with interbedded floodbasin deposits (FAs E and F).

The line of cross-section is roughly perpendicular to palaeoflow, and so the lensoid cross-

sectional geometries of Facies Association B bodies are realistic. A compensational stacking pattern is evident, in which successive channel bodies are preferentially located in zones unoccupied by prior channel deposits, exploiting palaeotopographic lows. At the location of the Frazer Beach measured section (Figs 10 and 12), no channel sandstone is present in the section until 18 m above the top of the VPC, providing an unusually fine-grained section. Elsewhere along the coastal section, FA B channel bodies are in erosional contact either with the top of the VPC or within 1 m of that level, suggesting a disconformable relationship from which the record of the terrestrial EPE event has likely been excised. It is, nonetheless, evident from these relationships that the top-VPC surface, historically regarded as recording both the EPE and PTB, is only locally disconformable.

Fluvial channel facies across this interface in Fig. 12 exhibit a somewhat fining-upward trend (dominantly FA A below, passing up into dominantly FA B above), contrary to the notion of fluvial 'rejuvenation' across the EPE and PTB (sensu Smith, 1995; Newell et al., 1999; Ward et al., 2000; Michaelsen, 2002; Arche & López-Gómez, 2005; Zhu et al., 2019, 2020). Preservation of sandstone and mudrock-dominated parttruncated by erosionally ings, based conglomerate beds within FA A bodies of the uppermost Permian succession, suggest that many if not all of these bodies are multistorey (Figs 4 and 8A). There are several recorded instances of large-scale (epsilon, sensu Allen, 1963) cross-bedding in FA A bodies across the Newcastle Coalfield (e.g. Diessel, 1992), and angular relationships between the dip direction of the macroform surfaces and those of dunescale cross-bedding indicate that the macroform cross-beds are indeed lateral accretion sets formed in 15 to 20 m deep, sand and gravel bed, meandering rivers. An example from the Upper Teralba Conglomerate in the field area is illustrated in Fig. 4A and B. In the Southern (Illawarra) Coalfield, channel bodies

uppermost Permian succession are sand-dominated, show no evidence of systematic lateral accretion, and are composed of mosaics of overlapping sheets and lenses (Fig. 4C). Channel bodies above the VPC in the Northern Coalfield and the equivalent Bulli Seam in the Southern Coalfield, are sandstone-dominated (FA B) and lack evidence of systematic lateral accretion (Figs 4D and 8A).

The lack of any significant change in fluvial style from the upper Permian to Lower Triassic in the Illawarra Coalfield, and the evidence of upward fining across the boundary in the Newcastle Coalfield, suggest that there was minimal change in fluvial style across the EPE in the Sydney Basin, Moreover, mean palaeoflow directions are consistent across the boundary in both areas (Fig. 13; and see Fielding et al., 2019) suggesting continuation of the same dispersal system following the EPE ponding event (Vajda et al., 2020), and reinforcing the notion that there was indeed no major change in the alluvial landscape after the disruption caused by the EPE ponding event. The basinwide pattern of palaeoflow records suggests that the central and eastern (preserved) parts of the basin were dominated by southward axial dispersal, whereas western regions were more dominated by transverse sediment dispersal from the cratonic landmass to the west. This pattern persists from the upper Permian into the lower Triassic succession (Fig. 13). The conglomeratic character of channel bodies in the uppermost Permian of the Newcastle Coalfield can be attributed to its more proximal location with respect to the sediment source (the emerging New England Orogen: Collins, 1991; Holcombe et al., 1997; Rosenbaum, 2018), and its location in the axial foredeep of a retroarc foreland basin as opposed to the cratonic basin margin context of the Illawarra Coalfield (Fig. 3: and see Fielding et al., 2001).

Petrographic examination of sandstone thinsections (Table 2) shows little if any change in quartz-feldspar-lithic fragment ratios across the EPE, indicating consistency in provenance

Fig. 14. Regional west to east cross-section spanning the entire Sydney Basin from the Western Coalfield near Lithgow to the Northern Coalfield near Newcastle, showing the variable expression of the end-Permian Extinction Event (EPE) and Permo-Triassic Boundary (PTB) across the basin. Across the eastern and central parts of the basin, the contact is broadly conformable (where the uppermost coal is overlain by mudrocks and heteroliths) to disconformable (where the uppermost coal is overlain by an erosionally based channel body). In the Western Coalfield, however, the contact becomes increasingly unconformable with excision of one or more uppermost Permian coal seams and their intervening strata (shown by the wavy red line). See Fig. 1 for line of section, and Fig. 12 for key to symbols and lithology colours used.

220 The Authors. Sedimentology © 2020 International Association of Sedimentologists, Sedimento

congruent with palaeoflow data. The dominantly litharenitic composition with a dominance of sedimentary rock fragments, for both upper Permian and Lower Triassic sands, suggests derivation predominantly from basement sources to the east and west of the Sydney Basin (New England Orogen and Lachlan Foldbelt, respectively).

Subsurface data

Subsurface mapping of uppermost Permian strata in the Newcastle Coalfield in combination with outcrop studies shows that channel bodies are composites of conglomerate and sandstone lithofacies, with individual storeys typically composed of one or other of Facies Associations A and B (Fig. 6). The proportion of conglomerate gradually, though irregularly, decreases upsection and across the EPE and PTB (Fig. 12). Furthermore, there are clearly multiple Facies Association A and B bodies in the succession, separated and enclosed by coal seam splits and thereby readily mapped. This is important, because a recent paper (Breckenridge et al., 2019) has posited that there is a single, regionally extensive erosion surface preserved within the Newcastle Coal Measures across the Newcastle Coalfield, separating sandstone-dominated upper delta plain strata below from conglomeratic alluvial plain strata above. It is clear, however, that Breckenridge et al. (2019, fig. 19) misidentified multiple erosion surfaces at different stratigraphic levels as the same surface. Given the correlations shown in Fig. 6, the stratigraphy is much more complex than implied by Breckenridge et al. (2019). There are, in fact, numerous erosionally based conglomerate and sandstonedominated bodies at various stratigraphic levels.

Maps of the three uppermost Permian channel bodies (Lower Teralba, Upper Teralba and Karignan conglomerates, respectively) and the lowermost 'Triassic' (post-VPC lower Munmorah Conglomerate) body have been compiled from a combination of surface and subsurface data (Tevvaw, 2019). All four bodies (Fig. 5) show clear, south-west-trending, linear plan geometries, with approximate widths of 5 to 10 km. South-westerly trends are consistent with palaeoflow data from outcrop (Fig. 5). All exhibit some curvature, and the Karignan Conglomerate map shows clear evidence for a major channel confluence (again, supported by palaeoflow data from outcrop). The zone of convergence between tributive two channels preserves

confluence scour fill that is locally over 50 m thick, a doubling in thickness over adjacent areas (Fig. 5). The locations of successive channel belts are offset from one another, indicating again that channel bodies preserve a compensational stacking pattern. The basal Triassic body is not as well-constrained because there are fewer drillholes where it is possible to propagate the correlations confidently (there being no coal seams or major tuffs in the basal Triassic section). The overwhelming south-westerly mode of dispersal shown by these maps (Fig. 5) and palaeoflow data (Fig. 13) indicates that sediment dispersal through what is now the Newcastle Coalfield was basin-axial, with little if any contribution from the presumed orogen to the east. The south-westerly modes from outcrop palaeoflow data sets are herein interpreted to all reflect axial dispersal, rather than an interference pattern between axial and transverse dispersal (Figs 3 and 13). At least some of the tuff beds show evidence of derivation from the east, however, suggesting that transverse supply of debris from explosive volcanic eruptions from time to time overwhelmed the axial fluvial systems. Axial sediment dispersal continued into the Early Triassic, although the frequency of volcanic eruptions seems to have declined dramatically across the PTB. Mapping of the basal Triassic Coal Cliff Sandstone by Diessel et al. (1967) and Dehghani (1994) in the Southern Coalfield confirms the south/south-westward (axial) dispersal pattern.

DISCUSSION

A cross-section from the western boundary of the Sydney Basin near Lithgow (Western Coalfield) to the east coast (Newcastle Coalfield) illustrates the changing nature of the EPE horizon's expression across the basin (Fig. 14). The EPE horizon has been most persistently removed by erosion in the Western Coalfield, where in many profiles a significant Permian section including the top (Katoomba) coal seam (for example, Wancol Lithgow-7; Fig. 14) has been excised. This horizon remains erosional but with less demonstrable relief across the central part of the transect, as far as AGL Bootleg-6, becoming more conformable to the east into the Newcastle Coalfield (for example, ELT Dooralong-8 and EHK Lisarow-1: Fig. 14). There are, nonetheless, locations where the EPE horizon is cryptic owing to post-depositional excision or non-formation of the uppermost coal (for example, DM Wyong-1: Fig. 14). The position of the PTB proper remains difficult to resolve in these sections owing to the scarcity of tuffs and radiogenic isotope ages above the EPE. Nevertheless, the available dates herein, complemented by palynostratigraphic correlation, suggest that the PTB lies, in most cases, within the initial mudrock to sandstone interval immediately above the EPE horizon.

Based on the combination of coastal outcrop data and borehole intersections, there are three expressions of the EPE horizon across the Sydney Basin; (i) unconformable (principally in the Western Coalfield); (ii) disconformable (sites scattered throughout the basin); and (iii) conformable (throughout much of the basin, with the exception of the Western Coalfield). The preponderance of disconformable to unconformable contacts in the Western Coalfield is probably a result of lower rates of accommodation and perhaps intermittent uplift along the western (cratonic) basin margin. Conversely, in the foredeep region of the Newcastle Coalfield, the boundary varies from disconformable to conformable, depending on whether a channel body was formed at a particular locality close to the time of the EPE. There is no evidence that the EPE horizon was regionally unconformable. There is, furthermore, no evidence of profound change in fluvial style across the boundary, with fluvial channel bodies of similar thickness, grain size and internal architecture below and above the boundary across almost the entire basin. The only exception to this is the abundance of very coarsegrained sandstones and conglomerates above the unconformable contact in parts of the Western Coalfield (for example, Wancol Putty-1: Fig. 14). This pattern becomes even more pronounced northward into the Gunnedah Basin, where the conglomeratic Digby Formation (Lower Triassic) unconformably overlies the upper Permian Black Jack Formation (Jian & Ward, 1993).

The character of the Permo-Triassic system boundary in the Sydney Basin contrasts with that interpreted from some other palaeocontinental regions where abrupt changes in fluvial style have been inferred (e.g. Smith, 1995; Newell *et al.*, 1999; Ward *et al.*, 2000; Michaelsen, 2002; Arche & López-Gómez, 2005; Zhu *et al.*, 2019, 2020). In the case of the Karoo Basin of southern Africa, researchers have recently provided more detailed logged sections that make a case for more gradual, progressive palaeo-environmental changes that are consistent with the findings of this study (e.g.

Smith & Botha-Brink, 2014; Botha et al., 2020). Moreover, uncertainties in the exact placement of the EPE and PTB render some of these examples open to speculation about the nature and timing of the boundaries (Gastaldo et al., 2020). It is possible that more distal locations within Permo-Triassic sedimentary basins in the region experienced the effects of end-Permian devegetation and consequent erosional flushing of sediment later than proximal locations. This would help to explain why the stratigraphy of the Sydney Basin preserves an unexpectedly muted response to the EPE.

Given the finding of Fielding et al. (2019) that the terrestrial EPE was not synchronous with the marine EPE or with the PTB in eastern Australia, it follows that cases where placement of the PTB has been based entirely on historical marine palaeobiological or biostratigraphical criteria cannot be considered well-constrained in absolute time. Resolution of the terrestrial EPE and the PTB in the Karoo Basin, for example, awaits wellconstrained ages close to those boundaries. In the recently published North China case (Zhu et al., 2019, 2020), the timing of events is constrained only by two maximum depositional ages from detrital zircon populations some (unspecified) distance apart (Zhu et al., 2019, fig. 2), and so the timing of reported palaeoenvironmental changes remains uncertain.

Notwithstanding these uncertainties, it is evident from the studies cited that the eastern Australian succession records less profound and more gradual change to the physical palaeoenvironment than has been disclosed from lower palaeolatitude sites despite the same abrupt extirpation of the flora. It is conceivable that changes in environmental parameters, such as surface temperature and soil moisture, were muted at higher palaeolatitudes, as has been predicted from climate simulation models (Kutzbach & Ziegler, 1993; Winguth et al., 2015; Penn et al., 2018). An increase in weathering indices has been noted at several sites in the Sydney Basin (Fielding et al., 2019) immediately above the EPE, at which level the Glossopteris flora disappears. This interval is also associated with spikes in Ni. High levels of heavy metal-bearing aerosols derived from either local or distant volcanic activity might have affected the regional vegetation or its symbiont mycoflora. If this was the cause of the terrestrial biotic crisis in the Sydney Basin, then there is no reason why the landscape would have been fundamentally affected, other than by the die-off of plant life.

CONCLUSIONS

The Permo-Triassic succession of the high southern palaeo-latitude Sydney Basin preserves a stratigraphically complete expression of the End-Permian Extinction (EPE) and the Permo-Triassic Boundary (PTB) in a lowland coastal alluvial plain setting. New absolute age constraints show that the terrestrial EPE, expressed by the disappearance of the Glossopteris flora, occurred some 600 to 200 kvr before the PTB and is recorded at the top of the uppermost coal seam of the Permian succession or in stratigraphically equivalent mudrocks of coastal plain floodbasin origin. An array of conglomeratedominated and sandstone-dominated channel belt bodies is preserved in the uppermost Permian succession, and mapping of channel belts suggests that various planform styles are represented. Following the initial ponding event at the EPE when standing water environments were widely developed, fluvial systems were reestablished at or about the time of the PTB.

The fluvial style of earliest Triassic coastal plain channel belt deposits, and interpreted sediment dispersal patterns, were little changed from those of the late Permian. The major upward change shown by the stratigraphy across the EPE is the complete loss of coal. A more gradual change towards better-drained alluvial landscapes is also manifest in a progressive shift to more coloured mudrocks, and the increasing abundance of desiccation structures, upward in the succession over tens of metres — an interval spanning hundreds of thousands to several million years. There is no evidence for a regionally developed rejuvenation of fluvial systems across the EPE, such as has been advocated in some other parts of the world and in eastern Australia by previous workers.

The nature of the stratigraphic contact at the EPE and PTB varies from place to place across the Sydney Basin. Over much of the basin, the transition across the EPE horizon is conformable to mildly disconformable, the latter exhibited where a post-EPE fluvial channel cut down through the floodbasin deposits of the EPE ponding event to locally rest directly on the uppermost coal seam. In the western part of the basin, however, the contact is more disconformable to unconformable, in response to tilting of the cratonic basin margin and greater levels of erosional downcutting. In parts of the Western Coalfield, this erosion has removed one or more of the uppermost Permian coal seams. This

erosion is, nonetheless, likely tectonically driven and unrelated to events at the EPE and PTB.

ACKNOWLEDGEMENTS

The research reported herein was funded by a collaborative research grant from the National Science Foundation (EAR-1636625 to C.F. and T.F.). Funding was also received from the Swedish Research Council (VR grant 2015-4264 to V.V. and VR grant 2014-5234 to S.M.). Referees P.B. Wignall, H.J. Song, and an anonymous individual, and Associate Editor Massimiliano Ghiprovided constructive reviews nassi, submitted manuscripts. We thank the staff at the W.B. Clarke Geoscience Centre in Londonderry, Sydney for facilitating access to the numerous drillcores used in this study. Justin Ahern drafted several of the illustrations.

CONFLICT OF INTEREST

The authors declare no conflicts of interest.

DATA AVAILABILITY STATEMENT

All data are provided in Tables and Supplementary Tables (Tables S1 and S2).

REFERENCES

- Adams, P.N., Slingerland, R.L. and Smith, N.D. (2004) Variations in natural levee morphology in anastomosed channel flood plain complexes. *Geomorphology*, 61, 127– 142.
- Algeo, T.J. and Twitchett, R.J. (2010) Anomalous Early Triassic sediment fluxes due to elevated weathering rates and their biological consequences. *Geology*, 38, 1023– 1026
- Algeo, T.J., Chen, Z.Q., Fraiser, M.L. and Twitchett, R.J. (2011) Terrestrial-marine teleconnections in the collapse and rebuilding of Early Triassic marine ecosystems. *Palaeogeogr. Palaeoclimatol. Palaeoecol.*, **308**, 1–11.
- Allen, J.R.L. (1963) The classification of cross-stratified units, with notes on their origin. Sedimentology, 2, 93– 114.
- Arche, A. and López-Gómez, J. (2005) Sudden changes in fluvial style across the Permian—Triassic boundary in the eastern Iberian Ranges, Spain: Analysis of possible causes. *Palaeogeogr. Palaeoclimatol. Palaeoecol.*, **229**, 104–126.
- Bamberry, W.J. (1990) Stratigraphy and sedimentology of the late Permian Illawarra Coal Measures, southern Sydney Basin, New South Wales. PhD thesis, University of Wollongong, 500 pp.

- Bamberry, W.J. and Herbert, C. (1996) Fluvial successions of the Late Permian to Triassic rocks of the northern Sydney Basin. Australasian Sedimentologists Group Field Guide Series, 9, 64 pp.
- Bamberry, W.J., Hutton, A.J. and Jones, B.G. (1995) The Permian Illawarra Coal Measures, southern Sydney Basin, Australia: a case study of deltaic sedimentation. In: Geology of Deltas (Eds Postma, G. and Oti, M.N.), A.A. Balkema, Rotterdam, 153–166.
- Benton, M.J. and Newell, A.J. (2014) Impacts of global warming on Permo-Triassic terrestrial ecosystems. Gondwana Res., 25, 1308–1337.
- Bercovici, A., Cui, Y., Forel, M.-B., Yu, J.X. and Vajda, V. (2015) Terrestrial palaeoenvironment characterization across the Permian-Triassic boundary in South China. *J. Asian Earth Sci.*, **98**, 225–246.
- Besly, B.M. and Fielding, C.R. (1989) Palaeosols in Westphalian coal-bearing and red-bed sequences, central and northern England. *Palaeogeogr. Palaeoclimatol. Palaeoecol.*, **70**, 303–330.
- Botha, J., Huttenlocker, A.K., Smith, R.M.H., Prevec, R., Viglietti, P. and Modesto, S.P. (2020) New geochemical and palaeontological data from the Permian-Triassic boundary in the South African Karoo Basin test the synchronicity of terrestrial and marine extinctions. *Palaeogeogr. Palaeoclimatol. Palaeoecol.*, **540**, 1–21.
- Bourquin, S., Rossignol, C., Jolivet, M., Poujol, M., Broutin, J. and Yu, J.X. (2018) Terrestrial Permian-Triassic boundary in southern China: new stratigraphic, structural and palaeoenvironment considerations. *Palaeogeogr. Palaeoclimatol. Palaeoecol.*, 490, 640–652.
- Bowring, S.A., Erwin, D.H., Jin, Y.G., Martin, M.W., Davidek, K. and Wang, W. (1998) U/Pb zircon geochronology and tempo of the end-Permian mass extinction. *Science*, **280**, 1039–1045.
- Breckenridge, J., Maravelis, A.G., Catuneanu, O., Ruming, K., Holmes, E. and Collins, W.J. (2019) Outcrop analysis and facies model of an Upper Permian tidally influenced fluvio-deltaic system: Northern Sydney Basin, SE Australia. Geol. Mag., 156, 1715–1741.
- Bridge, J.S. (1984) Large-scale facies sequences in alluvial overbank environments. J. Sed. Petrol., 54, 583–588.
- Brierley, G.J., Ferguson, R.J. and Woolfe, K.J. (1997) What is a fluvial levee? Sed. Geol., 114, 1–9.
- Brown, L.F. (1979) Deltaic sandstone facies of the Mid-Continent. In: Pennsylvanian Sandstones of the Mid-Continent (Ed. Hyne, N.J.), Tulsa Geol. Soc. Spec. Publ., 1, 35– 63.
- Burgess, S.D. and Bowring, S.A. (2015) High-precision geochronology confirms voluminous magmatism before, during, and after Earth's most severe extinction. Sci. Adv., 1, e1500470, 1–14.
- Burgess, S.D., Bowring, S.A. and Shen, S.-Z. (2014) High-precision timeline for Earth's most severe extinction. *Proc. Natl. Acad. Sci. USA*, 111, 3316–3321.
- Burns, C.E., Mountney, N.P., Hodgson, D.M. and Colombera, L. (2019) Stratigraphic architecture and hierarchy of fluvial overbank splay deposits. J. Geol. Soc. London, 176, 629–649.
- Campbell, I.H., Czamanske, G.K., Fedorenko, V.A., Hill, R.I. and Stepanov, V. (1992) Synchronism of the Siberian traps and the Permian-Triassic boundary. Science, 258, 1760–1763.
- Cao, C., Wang, W. and Jin, Y. (2002) Carbon isotope excursions across the Permian-Triassic boundary in the

- Meishan section, Zhejiang Province, China. *Chinese Sci. Bull.*, **47**, 1125–1129.
- Cao, C., Love, G.D., Hays, L.E., Wang, W., Shen, S. and Summons, R.E. (2009) Biogeochemical evidence for euxinic oceans and ecological disturbance presaging the end-Permian mass extinction event. *Earth Planet. Sci. Lett.*, 281, 188–201.
- Cas, R.A.F. and Wright, J.V. (1987) Volcanic Successions, Modern and Ancient. Allen and Unwin, London, 528 pp.
- Chu, D.L., Grasby, S.E., Song, H.J., Dal Corso, J., Wang, Y., Mather, T.A., Wu, Y.Y., Song, H.Y., Shu, W.C., Tong, J.N. and Wignall, P.B. (2020) Ecological disturbance in tropical peatlands prior to marine Permian-Triassic mass extinction. *Geology*, 48, 288–292.
- Clapham, M.E., Shen, S.Z. and Bottjer, D.J. (2009) The double mass extinction revisited: re-assessing the severity, selectivity, and paleobiogeographic pattern of the end-Guadalupian biotic crisis (Late Permian). *Paleobiology*, **35**, 32–50.
- Coalfield Geology Council of New South Wales (1999) Bulletin 1, 152 pp.
- Collins, W.J. (1991) A reassessment of the "Hunter-Bowen Orogeny": tectonic implications for the southern New England Fold Belt. Aust. J. Earth Sci., 38, 409–423.
- Collinson, J.W. and Isbell, J.L. (1984) Permian-Triassic sedimentology of the Beardmore Glacier region. Antarct. J. US, 21, 29–30.
- Collinson, J.W., Isbell, J.L., Elliot, D.H., Miller, M.F., Miller, J.M.G. and Veevers, J.J. (1994) Permian-Triassic Transantarctic basin. In: Permian-Triassic Pangean Basins and Foldbelts along the Panthalassan Margin of Gondwanaland (Eds Veevers, J.J. and Powell, C.McA.) Geol. Soc. Am. Memoir. 184, 173–222.
- Conaghan, P.J., Jones, J.G., McDonnell, K.L. and Royce, K. (1982) A dynamic fluvial model for the Sydney Basin. J. Geol. Soc. Aust., 29, 55–70.
- Cowan, E.J. (1993) Longitudinal fluvial drainage patterns within a foreland basin-fill: Permo-Triassic Sydney Basin, Australia. Sed. Geol., 85, 557–577.
- Dalrymple, R.W. and Choi, K. (2007) Morphologic and facies trends through the fluvial-marine transition in tidedominated depositional systems; a schematic framework for environmental and sequence stratigraphic interpretation. Earth-Sci. Rev., 81, 135–174.
- David, T.W.E. (1907) The geology of the Hunter River coal measures, New South Wales. Geol. Surv. NSW Mem. Geol., 4, 372.
- Davies, C., Allen, M.B., Busboy, M.M. and Safonova, I. (2010) Deposition in the Kuznetsk Basin, Siberia: insights into the Permian-Triassic transition and the Mesozoic evolution of central Asia. *Palaeogeogr. Palaeoclimatol. Palaeoecol.*, 295, 307–322.
- Dehghani, M.H. (1994) Sedimentology, genetic stratigraphy and depositional environment of the Permo-Triassic succession in the southern Sydney Basin, Australia. PhD thesis, University of Wollongong, 518 pp.
- Dickinson, W.R. (1983) Interpreting provenance relationships from detrital modes of sandstones. In: Provenance of Arenites (Ed. Zuffa, G.G.), NATO ASI Series, 148, 333–361.
- Diessel, C.F.K. (1980) Newcastle and Tomago coal measures. In: *A Guide to the Sydney Basin* (Eds Herbert, C. and Helby, R.), *Geol. Surv. NSW Bull.*, **26**, 101–114.
- Diessel, C.F.K. (1992) Coal-Bearing Depositional Systems pp. 721 Springer-Verlag, Berlin.

- Diessel, C.F.K. and Moelle, K.H.R. (1965) The application of analysis of the sedimentary and structural features of a coal seam and its surrounding strata to the operations of mining. 8th Commonwealth Mining and Metallurgical Congress, Melbourne, Proc., 6, 837–859.
- Diessel, C.F.K., Driver, R.C. and Moelle, K.H.R. (1967) Some geological investigations into a fossil river system in the roof strata of the Bulli Seam, Southern Coalfield, N.S.W. Proc. Austr. Inst. Min. Metall., 221, 19–37.
- Duchaufour, P. (1982) *Pedology*. Allen and Unwin, London, 448 pp.
- Elliot, D.H., Fanning, C.M., Isbell, J.L. and Hulett, S.R.W. (2017) The Permo-Triassic Gondwana sequence, central Transantarctic Mountains, Antarctica: Zircon geochronology, provenance, and basin evolution. *Geosphere*, 13, 155–178.
- Elliott, T. (1974) Interdistributary bay sequences and their genesis. *Sedimentology*, **21**, 611–622.
- Erwin, D.H. (2006) Extinction: How Life on Earth Nearly Ended 250 Million Years Ago. Princeton University Press, Princeton, NJ, 296 pp.
- Ethridge, F.G., Skelly, R.L. and Bristow, C.S. (1999)
 Avulsion and crevassing in the sandy, braided Niobrara
 River: complex response to base-level rise and
 aggradation. In: Fluvial Sedimentology VI (Eds Smith, N.D.
 and Rogers, J.), International Association of
 Sedimentologists Special Publication, 39, 179–191.
- Facer, R.A. and Foster, C.B. (Eds) (2003) Geology of the Cranky Corner Basin. Geol. Surv. NSW Coal Petrol. Bull., 4, 252.
- Farrell, K.M. (2001) Geomorphology, facies architecture, and high-resolution, non-marine sequence stratigraphy in avulsion deposits, Cumberland Marshes, Saskatchewan. Sed. Geol., 139, 93–150.
- Fielding, C.R. (1984) Upper delta plain lacustrine and fluviolacustrine facies from the Westphalian of the Durham coalfield, NE England. Sedimentology, 31, 547– 567.
- Fielding, C.R. (1986) Fluvial channel and overbank deposits from the Westphalian of the Durham coalfield, NE England. Sedimentology, 33, 119–140.
- Fielding, C.R. (2015) A reappraisal of large, heterolithic channel fills in the upper Permian Rangal Coal Measures of the Bowen Basin, Queensland, Australia: the case for tidal influence. In: Fluvial-tidal Sedimentology (Eds Ashworth, P.J., Best, J.L., and Parsons, D.R.), Developments in Sedimentology Series, Elsevier Science, 68, 323–351.
- Fielding, C.R., Falkner, A.J. and Scott, S.G. (1993) Fluvial response to foreland basin overfilling: the Late Permian Rangal Coal Measures in the Bowen Basin, Queensland, Australia. Sed. Geol., 85, 475–497.
- Fielding, C.R., Stephens, C.J. and Holcombe, R.J. (1997)
 Permian stratigraphy and palaeogeography of the eastern
 Bowen Basin, Gogango Overfolded Zone and Strathmuir
 Synclinorium in the Rockhampton-Mackay region, central
 Queensland. In: Tectonics and Metallogenesis of the New
 England Orogen (Eds Ashley, P.M. and Flood, P.G.), Spec.
 Publ. Geol. Soc. Aust., 19, 80–95.
- Fielding, C.R., Sliwa, R., Holcombe, R.J. and Jones, A.T. (2001) A new palaeogeographic synthesis for the Bowen, Gunnedah and Sydney Basins of eastern Australia. In: Eastern Australasian Basins Symposium, A Refocused Energy Perspective for the Future (Eds Hill, K.C. and

- Bernecker, T.), Spec. Publ. Petrol. Expln. Soc. Aust., Perth, W.A., 269–278.
- Fielding, C.R., Alexander, J. and Allen, J.P. (2018) The role of discharge variability in the formation and preservation of alluvial sediment bodies. Sed. Geol., 365, 1–20.
- Fielding, C.R., Frank, T.D., McLoughlin, S., Vajda, V., Mays, C., Tevyaw, A.P., Winguth, A., Winguth, C., Nicoll, R.S., Bocking, M. and Crowley, J.L. (2019) Age and pattern of southern high-latitude continental end-Permian extinction constrained by multiproxy analysis. Nat. Commun., 10, 385.
- Filguera-Rivera, M., Smith, N.D. and Slingerland, R.L. (2007) Controls on natural levee development in the Columbia River, British Columbia, Canada. Sedimentology, 54, 905–919.
- Folk, R.L. (1980) Petrology of Sedimentary Rocks. Hemphill Pub. Co., Austin, TX, 184 pp.
- Gastaldo, R.A. and Neveling, J. (2016) Comment on: "Anatomy of a mass extinction: Sedimentological and taphonomic evidence for drought-induced die-offs at the Permo-Triassic boundary in the main Karoo Basin, South Africa" by R.M.H. Smith and J. Botha-Brink. *Palaeogeogr. Palaeoclimatol. Palaeoecol.*, 447, 88–91.
- Gastaldo, R.A., Kamo, S.L., Neveling, J., Geissman, J.W., Bamford, M. and Looy, C.V. (2015) Is the vertebratedefined Permian-Triassic boundary in the Karoo Basin, South Africa, the terrestrial expression of the end-Permian marine event? Geology, 43, 939–942.
- Gastaldo, R.A., Neveling, J., Geissman, J.W. and Kamo, S.L. (2018) A lithostratigraphic and magnetostratigraphic framework in a geochronologic context for a purported Permian-Triassic boundary section at Old (West) Lootsberg Pass, Karoo Basin, South Africa. *Geol. Soc. Am. Bull.*, 130, 1411–1438.
- Gastaldo, R.A., Kamo, S.L., Neveling, J., Geissman, J.W., Looy, C.V. and Martin, A.M. (2020) The base of the Lystrosaurus Assemblage Zone, Karoo Basin, predates the end-Permian marine extinction. Nat. Commun., 11, 1428.
- Gingras, M.K. and MacEachern, J.A. (2012) Tidal ichnology of shallow-water clastic settings. In: *Principles of Tidal Sedimentology* (Eds Davis R.A. and Dalrymple, R.W.), pp. 57–77. Springer, Berlin.
- Gingras, M.K., MacEachern, J.A. and Dashtgard, S.E. (2011) Process ichnology and the elucidation of physico-chemical stress. Sed. Geol., 237, 115–134.
- Glasspool, I.J. and Scott, A.C. (2010) Phanerozoic concentrations of atmospheric oxygen reconstructed from sedimentary charcoal. *Nature Geosci.*, 3, 627–630.
- Glen, R.A. (2005) The Tasmanides of eastern Australia. In: Terrane Processes at the Margins of Gondwana (Eds Vaughan, A.P.M., Leat, P.T. and Pankhurst, R.J.), Spec. Publ. Geol. Soc. London, 246, 23–96.
- **Goldbery**, **R.** and **Holland**, **W.N.** (1973) Stratigraphy and sedimentation of redbed facies in Narrabeen Group of Sydney Basin, Australia. *AAPG Bull.*, **57**, 1314–1334.
- Grasby, S.E., Sanei, H. and Beauchamp, B. (2011) Catastrophic dispersion of coal fly ash into oceans during the latest Permian extinction. *Nature Geosci.*, 4, 104–107.
- Harwood, G. (1988) Microscopical techniques: II. Principles of sedimentary petrography. In: Techniques in Sedimentology (Ed. Tucker, R.M.), pp. 108–173. Blackwell Science, Oxford.
- Herbert, C. and Helby, R. (Eds) (1980) A guide to the Sydney Basin. Geol. Surv. NSW Bull., 26, 603.

- Holcombe, R.J., Stephens, C.J., Fielding, C.R., Gust, D.A.,
 Little, T.A., Sliwa, R., Kassan, J., McPhie, J. and Ewart, A.
 (1997) Tectonic evolution of the northern New England
 Fold Belt: The Permian-Triassic Hunter-Bowen event. In:
 Tectonics and Metallogenesis of the New England Orogen
 (Eds Ashley, P.M. and Flood, P.G.), Spec. Publ. Geol. Soc.
 Aust., 19, 52-65.
- Isozaki, Y., Kawahata, H. and Ota, A. (2007a) A unique carbon isotope record across the Guadalupian-Lopingian (Middle-Upper Permian) boundary in mid-oceanic paleoatoll carbonates: the high-productivity) Kamura Event" and its collapse in Panthalassa. Global Planet. Change, 55, 21–38.
- Isozaki, Y., Kawahata, H. and Minoshima, K. (2007b) The Capitanian (Permian) Kamura cooling event: the beginning of the Paleozoic-Mesozoic transition. *Palaeoworld*, 16, 16– 30.
- Jian, F.X. and Ward, C.R. (1993) Triassic depositional episode. In: The Gunnedah Basin, New South Wales (Ed. Tadros, N.Z.), Geol. Surv. NSW, Memoir Geology, 12, 297–326.
- Jiang, H.S., Joachimski, M.M., Wignall, P.B., Zhang, M.H. and Lai, X.L. (2015) A delayed end-Permian extinction in deep-water locations and its relationship to temperature trends (Bianyang, Guizhou Province, South China). Palaeogeogr. Palaeoclimatol. Palaeoecol., 440, 690–695.
- Jorgensen, P.J. and Fielding, C.R. (1996) Facies architecture of alluvial floodbasin deposits: three-dimensional data from the Upper Triassic Callide Coal Measures of eastcentral Queensland, Australia. Sedimentology, 43, 479– 495.
- Jorgensen, P.J. and Fielding, C.R. (1999) Debris-flow deposits in an alluvial-plain succession: the Upper Triassic Callide Coal Measures of Queensland, Australia. J. Sed. Res., 69, 1027–1040.
- Kamo, S.L., Czamanske, G.K., Amelin, Y., Fedorenko, V.A., Davis, D.W. and Trofimov, V.R. (2003) Rapid eruption of Siberian flood-volcanic rocks and evidence for coincidence with the Permian-Triassic boundary and mass extinction at 251 Ma. Earth Planet. Sci. Lett., 214, 75–91.
- Kiehl, J.T. and Shields, C.A. (2005) Climate simulation of the latest Permian: implications for mass extinction. *Geology*, **33**, 757–760.
- Korsch, R.J. and Totterdell, J.M. (2009) Subsidence history and basin phases of the Bowen, Gunnedah and Surat Basins, eastern Australia. Aust. J. Earth Sci., 56, 335–353.
- Kutzbach, J.E. and Gallimore, R.G. (1989) Pangean climates: megamonsoons of the megacontinent. J. Geophys. Res., 94, 3341–3357.
- Kutzbach, J.E. and Ziegler, A.M. (1993) Simulation of Late Permian climate and biomes with an atmosphere-ocean model: comparisons with observations. *Phil. Trans. Roy.* Soc. London, Series B, 341, 327–340.
- Laurie, J.R., Bodorkos, S., Nicoll, R.S., Crowley, J.L., Mantle, D.J., Mory, A.J., Wood, G.R., Backhouse, J., Holmes, E.K., Smith, T.E. and Champion, D.C. (2016) Calibrating the middle and late Permian palynostratigraphy of Australia to the geologic time-scale via U-Pb zircon CA-IDTIMS dating. *Aust. J. Earth Sci.*, **63**, 701–730.
- Le Vaillant, M., Barnes, S.J., Mungall, J.E. and Mungall, E.L. (2017) Role of degassing of the Noril'sk nickel deposits in the Permian-Triassic mass extinction event. *Proc. Natl. Acad. Sci. USA*, 114, 2485–2490.

- Lopez-Gomez, J., Arche, A., Marzo, M. and Durand, M. (2005) Stratigraphical and palaeogeographical significance of the continental sedimentary transition across the Permian-Triassic boundary in Spain. *Palaeogeogr. Palaeoclimatol. Palaeoecol.*, **229**, 3–23.
- MacEachern, J.A. and Gingras, M.K. (2007) Recognition of brackish-water trace-fossil suites in the Cretaceous Western Interior Seaway of Alberta, Canada. In: Sediment-Organism Interactions: A Multifaceted Ichnology (Eds Bromley, R., Buatois, L.A., Genise, J., Mangano, M.G. and Melchor, R.), SEPM Spec. Publ., 88, 149–194.
- Martinius, A.W. and van den Berg, J.H. (2011) Atlas of sedimentary structures in estuarine and tidally-influenced river deposits of the Rhine-Meuse-Scheldt system: Their application to the interpretation of analogous outcrop and subsurface depositional systems. EAGE, Houten, 298 pp.
- Mayne, S.J., Nicholas, E., Bigg-Wither, A.L., Rasidi, J.S. and Raine, M.J. (1974) Geology of the Sydney Basin a review. *Bull. Bur. Mineral Resour. Geol. Geophys.*, **149**, 229 pp.
- Mays, C., Vajda, V., Fielding, C., Frank, T., Tevyaw, A. and McLoughlin, S. (2020) Refined Permian–Triassic floristic timeline reveals early collapse and delayed recovery of south polar terrestrial ecosystems. GSA Bull., 132, 1489– 1513.
- McLoughlin, S. and Drinnan, A.N. (1997a) Revised stratigraphy of the Permian Bainmedart Coal Measures, northern Prince Charles Mountains, East Antarctica. Geol. Mag., 134, 335–353.
- McLoughlin, S. and Drinnan, A.N. (1997b) Fluvial sedimentology and revised stratigraphy of the Triassic Flagstone Bench Formation, northern Prince Charles Mountains, East Antarctica. *Geol. Mag.*, **134**, 781–806.
- McLoughlin, S., Mays, C., Vajda, V., Bocking, M., Frank, T.D. and Fielding, C.R. (in press) Dwelling in the dead zone vertebrate burrows immediately succeeding the end-Permian extinction event in Australia. *Palaios*. https://doi.org/10.2110/palo.2020.007
- McLoughlin, S., Lindström, S. and Drinnan, A.N. (1997) Gondwanan floristic and sedimentological trends during the Permian-Triassic transition: new evidence from the Amery Group, northern Prince Charles Mountains, East Antarctica. *Antarct. Sci.*, **9**, 281–298.
- McLoughlin, S., Maksimenko, A. and Mays, C. (2019) A new high-paleolatitude permineralized peat flora from the late Permian of the Sydney Basin, Australia. *Intl. J. Plant Sci.*, **180**, 513–539.
- Metcalfe, I., Crowley, J.L., Nicoll, R.S., and Schmitz, M. (2015) High-precision U-Pb CA-TIMS calibration of Middle Permian to Lower Triassic sequences, mass extinction and extreme climate-change in eastern Australian Gondwana. *Gondwana Res.*, 28, 61–81.
- Michaelsen, P. (2002) Mass extinction of peat-forming plants and the effect on fluvial styles across the Permian-Triassic boundary, northern Bowen Basin, Australia. *Palaeogeogr. Palaeoclimatol. Palaeoecol.*, **179**, 173–188.
- Moloney, J., Beckett, J. and Holmes, G.G. (1991) Coal. In: Geology of the Camberwell, Dungog, and Bulahdelah 1:100,000 Sheets (Eds Roberts, J., Engel, B., and Chapman, J.), Geol. Surv. NSW, 382.
- Newell, A.J., Tverdokhlebov, V.P. and Benton, M.J. (1999) Interplay of tectonics and climate on a transverse fluvial system, Upper Permian, southern Uralian Foreland Basin, Russia. Sed. Geol., 127, 11–29.

- Newhall, C.G. and Punongbayan, R.S. (Eds) (1996) Fire and Mud, Eruptions and Lahars of Mount Pinatubo, Philippines. Philippine Institute of Volcanology and Seismology, Quezon City and University of Washington Press, Seattle, 1126 pp.
- Ogg, J.G., Ogg, G.M. and Gradstein, F.M. (2016) A Concise Geologic Time Scale. Elsevier Science, Amsterdam, 234 pp.
- Payne, J.L. and Kump, L.R. (2007) Evidence for recurrent Early Triassic massive volcanism from quantitative interpretation of carbon isotope fluctuations. *Earth Planet. Science Lett.*, 256, 264–277.
- Penn, J.L., Deutsch, C., Payne, J.L. and Sperling, E.A. (2018) Temperature-dependent hypoxia explains biogeography and severity of end-Permian marine mass extinction. *Science*, **362**, eaat1327.
- Perez-Arlucea, M. and Smith, N.D. (1990) Depositional patterns following the 1870s avulsion of the Saskatchewan River (Cumberland Marshes, Saskatchewan, Canada). *J. Sed. Res.*, **69**, 62–73.
- Pigg, K.B. and McLoughlin, S. (1997) Anatomically preserved Glossopteris leaves from the Bowen and Sydney basins, Australia. Rev. Palaeobot. Palynol., 97, 339–359.
- Pratt, G.W. (2010) A revised Triassic stratigraphy for the Lorne Basin, NSW. Quart. Notes Geol. Surv. NSW, 134, 1–35.
- Price, P.L. (1997) Permian to Jurassic palynostratigraphic nomenclature of the Bowen and Surat basins. In: *The* Surat and Bowen Basins, Southeast Queensland (Ed. Green, P.M.), pp. 137–178. Queensland Department of Mines and Energy, Brisbane, Australia.
- Rampino, M.R. and Shen, S.-Z. (2020) The end-Guadalupian (259.8 Ma) biodiversity crisis: the sixth major mass extinction? *Hist. Biol.*, 1–7. https://doi.org/10.1080/08912963.2019.1658096
- Rampino, M.R., Rodriguez, S., Baransky, E. and Cai, Y. (2017) Global nickel anomaly links Siberian Traps eruptions and the latest Permian mass extinction. *Sci. Rep.*, 7, 12416.
- Renne, P.R. and Basu, A.R. (1991) Rapid eruption of the siberian traps flood basalts at the permo-triassic boundary. Science, 253, 176–179.
- Renne, P.R., Zichao, Z., Richards, M.A., Black, M.T. and Basu, A.R. (1995) Synchrony and causal relations between Permian-Triassic boundary crisis and Siberian flood volcanism. Science, 269, 1414–1416.
- Retallack, G.J. (1999) Postapocalyptic greenhouse paleoclimate revealed by earliest Triassic paleosols in the Sydney Basin, Australia. *Geol. Soc. Am. Bull.*, **111**, 52–70.
- Retallack, G.J. (2005) Earliest Triassic claystone breccias and soil-erosion crisis. J. Sed. Res., 75, 679–695.
- Retallack, G.J. (2013) Permian and Triassic greenhouse crises. Gond. Res., 24, 90–103.
- Retallack, G.J. and Jahren, A.H. (2008) Methane release from igneous intrusion of coal during Late Permian extinction events. *J. Geol.*, 116, 1–20.
- Retallack, G.J., Jahren, A.H., Sheldon, N.D., Chakrabarti, R., Metzger, C.A. and Smith, R.M.H. (2005) The Permian-Triassic boundary in Antarctica. Antarct. Sci., 17, 241–258.
- Retallack, G.J., Sheldon, N.D., Carr, P.F., Fanning, M., Thompson, C.A., Williams, M.L., Jones, B.G. and Hutton, A. (2011) Multiple Early Triassic greenhouse crises impeded recovery from Late Permian mass extinction. Palaeogeogr. Palaeoclimatol. Palaeoecol., 308, 233–251.
- Rosenbaum, G. (2018) The Tasmanides: phanerozoic tectonic evolution of eastern Australia. Annu. Rev. Earth Planet. Sci., 46, 291–325.

- Rothman, D.H., Fournier, G.P., French, K.L., Alm, E.J., Boyle, E.A., Cao, C.Q. and Summons, R.E. (2014) Methanogenic burst in the end-Permian carbon cycle. *Proc. Natl. Acad. Sci. USA*, 111, 5462–5467.
- Scheibner, E. (1973) A plate tectonic model of the Palaeozoic tectonic history of New South Wales. J. Geol. Soc. Aust., 20, 405–426.
- Scheibner, E. (1993) Tectonic setting. In: The Gunnedah Basin, New South Wales (Ed. Tadros, N.Z.) Mem. Geol. Surv. NSW, 12, 33–46.
- Shen, S.Z., Crowley, J.L., Wang, Y., Bowring, S.A., Erwin, D.H., Sadler, P.M., Cao, C.Q., Rothman, D.H., Henderson, C.M., Ramezani, J., Zhang, H., Shen, Y.N., Liu, X.L., Liu, L.J., Zeng, Y., Jiang, Y.F. and Jin, Y.G. (2011) Calibrating the end-Permian mass extinction. *Science*, 334, 1367–1372.
- Smith, R.M.H. (1995) Changing fluvial environments across the Permo-Triassic boundary in the Karoo Basin, South Africa and possible causes of tetrapod extinctions. Palaeogeogr. Palaeoclimatol. Palaeoecol., 117, 81–104.
- Smith, R.M.H. and Botha-Brink, J. (2014) Anatomy of a mass extinction: sedimentological and taphonomic evidence for drought-induced die-offs at the Permo-Triassic boundary in the main Karoo Basin, South Africa. *Palaeogeogr. Palaeoclimatol. Palaeoecol.*, 396, 99–118.
- Sobolev, S.V., Sobolev, A.V., Kuzmin, D.V., Krivolutskaya, N.A., Petrunin, A.G., Arndt, N.T., Radko, V.A. and Vasiliev, Y.R. (2011) Linking mantle plumes, large igneous provinces and environmental catastrophes. *Nature*, 477, 312–316.
- Song, H., Wignall, P.B., Tong, J. and Yin, H. (2013) Two pulses of extinction during the Permian-Triassic crisis. *Nature Geosci.*, **6**, 52–56.
- Stanley, S.M. and Yang, X. (1994) A double mass extinction at the end of the Paleozoic era. *Science*, **266**, 1340–1344.
- Svensen, H., Planke, S., Polozov, A.G., Schmidbauer, N., Corfu, F., Podladchikov, Y.Y. and Jamtveit, B. (2009) Siberian gas venting and the end-Permian environmental crisis. *Earth Planet. Sci. Lett.*, **277**, 490–500.
- Tabor, N.J., Myers, T.S. and Michel, L.A. (2017) Sedimentologist's guide for recognition, description, and classification of paleosols. In: Terrestrial Depositional Systems: Deciphering Complexities through Multiple Stratigraphic Methods (Eds Zeigler, K.E. and Parker, W.G.), pp. 165–208. Elsevier Science, Amsterdam.
- **Tevyaw, A.P.** (2019) Expression of the Permo-Triassic boundary in a high accommodation, high southern paleolatitude continental margin setting. Master of Science thesis, University of Nebraska-Lincoln, 81 pp.
- Torsvik, T.H. and Cocks, L.R.M. (2013) Gondwana from top to base in space and time. *Gond. Res.*, **24**, 999–1030.
- Tye, R.S. and Coleman, J.M. (1989) Evolution of Atchafalaya lacustrine deltas. Sed. Geol., 65, 95–112.
- Tye, S.C., Fielding, C.R. and Jones, B.G. (1996) Stratigraphy and sedimentology of the Permian Talaterang and Shoalhaven Groups in the southernmost Sydney Basin, New South Wales. *Aust. J. Earth Sci.*, **43**, 57–69.
- Uren, R. (1980) Notes on the Clifton Sub-Group, northeastern Sydney Basin. In: A Guide to the Sydney Basin (Eds Herbert, C. and Helby, R.), Geol. Surv. NSW Bull., 26, 162–168.
- Vajda, V., McLoughlin, S., Mays, C., Fielding, C.R., Tevyaw, A., Lehsten, V., Bocking, M. and Nicoll, R.S. (2020) End-Permian (252 Mya) deforestation, wildfires and flooding—

- An ancient biotic crisis with lessons for the present. Earth Planet. Sci. Lett., 529, 115875, 1-13.
- Vallance, J.W. and Scott, K.M. (1997) The Osceola Mudflow from Mount Rainier: sedimentology and hazard implications of a huge clay-rich debris flow. Geol. Soc. Am. Bull., 109, 143-163.
- Veevers, J.J. (2000) Permian-Triassic Pangean basins and fold belts along the Panthalassan margin of eastern Australia. In: Billion-Year Earth History of Australia and Neighbours in Gondwanaland (Ed. Veevers, J.J.), pp. 235-252. GEMOC Press, Sydney, Australia.
- Warbrooke, P.R. (1981) Depositional environments of the upper Tomago and lower Newcastle Coal Measures, New South Wales. PhD thesis, University of Newcastle, 265 pp.
- Ward, C.R. (1972) Sedimentation in the Narrabeen Group, southern Sydney Basin, New South Wales. J. Geol. Soc. Aust., 19, 393–409.
- Ward, P.D., Montgomery, D.R. and Smith, R. (2000) Altered river morphology in South Africa related to the Permian-Triassic extinction. Science, 289, 1740–1743.
- Webb, J.A. and Fielding, C.R. (1993) Permo-Triassic sedimentation within the Lambert Graben, northern Prince Charles Mountains, East Antarctica, In: Gondwana Eight: Assembly, Evolution and Dispersal (Eds Findlay, R.H., Unrug, R., Banks, M.R. and Veevers, J.J.), pp. 357-369. A.A. Balkema, Rotterdam.
- Weber, C.R. and Smith, B.C. (2001) Stratford Coal Bed Methane Prospect, PEL 285, Gloucester Basin, New South Wales, Review of Exploration Results and Resource Estimate. Pacific Power International Report, 92 pp. Accessed via New South Wales Government DIGS database.
- Wheeler, A., Van de Wetering, N., Esterle, J.S. and Gotz, A.E. (2020) Palaeoenvironmental changes recorded in the palynology and palynofacies of a Late Permian Marker Mudstone (Galilee Basin, Australia). Paleoworld, 29, 435-452.
- Wignall, P.B. (2001) Large igneous provinces and mass extinctions. Earth-Sci. Rev., 53, 1-33.
- Wignall, P.B., Chu, D.L., Hilton, J.M., Dal Corso, J., Wu, Y.Y., Wang, Y., Atkinson, J. and Tong, J.N. (2020) Death in the shallows: the record of Permo-Triassic mass extinction in paralic settings, southwest China. Global Planet. Change, 189, 103176, 1-12.
- Winguth, A.M.E., Shields, C. and Winguth, C. (2015) Transition into a hothouse world at the Permian-Triassic boundary - a model study. Palaeogeogr. Palaeoclimatol. Palaeoecol., 440, 316-327.
- Yago, J.V.R. and Fielding, C.R. (2015) Depositional environments and sediment dispersal patterns of the Jurassic Walloon Subgroup in eastern Australia. In: Eastern Australasian Basins Symposium, a Powerhouse Emerges; Energy for the Next Fifty Years (Ed. Lodwick, W.), Petroleum Exploration Society of Australia Special Publication, 141–150.
- Yan, Z.M., Shao, L.Y., Glasspool, I.J., Wang, J., Wang, X.T. and Wang, H. (2019) Frequent and intense fires in the

- final coals of the Paleozoic indicate elevated atmospheric oxygen levels at the onset of the End-Permian Mass Extinction Event. Int. J. Coal Geol., 207, 75-83.
- Yang, W., Feng, Q., Liu, Y.Q., Tabor, N., Miggins, D., Crowley, J.L., Lin, J.Y. and Thomas, S.G. (2010) Depositional environments and cyclo- and chronostratigraphy of uppermost Carboniferous - Lower Triassic fluvial-lacustrine deposits, southern Bogda Mountains, NW China - a terrestrial paleoclimatic record of mid-latitude NE Pangea. Global Planet. Change, 73, 15-113.
- Yin, H.F., Zhang, K.X., Tong, J.N., Yang, Z.Y. and Wu, S.B. (2001) The Global Stratotype Section and Point (GSSP) of the Permian-Triassic boundary. Episodes, 24, 102-114.
- Yin, H.F., Tong, J.N. and Zhang, K.X. (2005) A review on the Global Stratotype Section and Point of the Permian-Triassic boundary. Acta Geol. Sinica, 79, 715–728.
- Yin, H.F., Feng, Q.L., Lai, X.L., Baud, A. and Tong, J.N. (2007) The protracted Permo-Triassic crisis and the multiact mass extinction around the Permian-Triassic boundary. Global Planet. Change, 55, 1-20.
- Yu, J.X., Peng, Y.Q., Zhang, S.X., Yang, F.Q., Zhao, Q.M. and Huang, Q.S. (2007) Terrestrial events across the Permian-Triassic boundary along the Yunnan-Guizhou border, SW China. Global Planet. Change, 55, 193-208.
- Zhu, Z.C., Liu, Y.Q., Kuang, H.W., Benton, M.J., Newell, A.J., Xu, H., An, W., Ji, S., Xu, S.C., Peng, N. and Zhai, Q.G. (2019) Altered fluvial patterns in North China indicate rapid climate change linked to the Permian-Triassic mass extinction. Sci. Rep., 9, 16818.
- Zhu, Z.C., Kuang, H.W., Liu, Y.Q., Benton, M.J., Newell, A.J., Xu, H., An, W., Ji, S.A., Xu, S.C., Peng, N. and Zhai, Q.G. (2020) Intensifying aeolian activity following the end-Permian mass extinction: Evidence from the Late Permian-Early Triassic terrestrial sedimentary record of the Ordos Basin, North China. Sedimentology, 67, 2691-2720.

Manuscript received 9 April 2020; revision 30 June 2020; revision accepted 10 July 2020

Supporting Information

Additional information may be found in the online version of this article:

- Table S1. LA-ICPMS isotopic U-Pb and trace element concentration data.
 - **Table S2.** CA-TIMS zircon U-Pb isotopic data.
- Data S1. Further details of LA-ICPMS and CA-TIMS methods, and results.
- Figure S1. CL images of zircon. Grains dated by
- CA-TIMS are identified by yellow labels z1, z2, etc. Figure S2. Plot of ²⁰⁶Pb/²³⁸U dates obtained by CA-TIMS. Plotted with Isoplot 3.0 (Ludwig, 2003).